HPLC ANALYSIS OF PHENOLIC COMPOUNDS FROM ARTEMISIA SPECIES

Bianca Ivanescu,[a]* Laurian Vlase,[b] Cristina Lungu[a] and Andreia Corciova[c]

Keywords: Methoxylated flavones, antioxidant, *Artemisia annua*, *Artemisia vulgaris*, *Artemisia absinthium*

The aim of this study was the identification and quantification of biologically active compounds from three *Artemisia* species, used as remedies in Romanian traditional medicine. A new LC-MS method was developed for the analysis of methoxylated flavones and also the quantification of caffeic and chlorogenic acids was performed. The antioxidant activity of plant extracts was evaluated by DPPH radical scavenging assay. We report for the first time the presence of eupatorin and hispidulin in *A. absinthium* and *A. vulgaris*, of eupatilin in *A. annua* and casticin in *A. vulgaris*. Jaceosidin and acacetin were not identified in any sample. Although all extracts showed antiradical scavenging activity, *A. vulgaris* exhibited the strongest antioxidant effect. Chlorogenic acid was found in high amounts in all species, notably in *A. annua* and *A. vulgaris*.

* Corresponding Authors
Fax: +40.232.211.820
E-Mail: biancaivanescu@yahoo.com
[a] "Grigore T. Popa" University of Medicine and Pharmacy Iasi, Faculty of Pharmacy, Department of Pharmaceutical Botany, 16 Universitatii Street, 700115 Iasi, Romania
[b] "IuliuHatieganu" University of Medicine and Pharmacy, Faculty of Pharmacy, Department of Pharmaceutical Technology and Biopharmacy, 12 Ion Creanga Street, 400010 Cluj-Napoca, Romania
[c] "Grigore T. Popa" University of Medicine and Pharmacy Iasi, Faculty of Pharmacy, Department of Drugs Analysis, 16 Universitatii Street, 700115 Iasi, Romania

Introduction

Polyphenolic compounds constitute one of the largest, most widely spread and functionally important groups of secondary plant metabolites. In recent years, these substances, and flavonoids in particular, have attracted great interest due to their antioxidant capacity which confers them a valuable therapeutic potential in treating free-radical mediated diseases. Plant polyphenols are serious candidates in explanations of the protective effects of plants against cancer and cardiovascular maladies.

Although medicinal plants stood the test of time as traditional remedies, their phytochemistry is only partially known. The species selected for this study have long been used in Romania as herbal medicines, but also throughout the world and are included in the pharmacopoeias of different countries.[1] *Artemisia annua* L., *Artemisia absinthium* L. and *Artemisia vulgaris* L. (*Asteraceae* family) are largely spread in nature and employed in the treatment of various conditions, such as hepatitis, inflammation, bacterial and fungal infections, cancer, malaria, helminthiasis and other parasitic infections.[2] *A. annua* became known globally after the identification and isolation of the antimalarial compound artemisinin and today is investigated for its anticancer compounds.[3]

Many of the above mentioned pharmacological activities are due to the phenolic compounds present in the plants and for this reason, the present study focuses on them. This research continues the work from a previously published study that examined the occurrence of 18 phenolic compounds in the same *Artemisia* species.[4] The present paper is centred on the analysis of six methoxylated flavones, valuable bioactive compounds with numerous therapeutic properties, mainly antitumor, anti-inflammatory, antioxidant, antimicrobial and anti-ulcer.[4-7] For this purpose, a new LC-MS method was developed and applied to the plant extracts in order to identify and quantify the methoxylated flavones in the tested species. Because in the previous study, caffeic and chlorogenic acids were only identified, but not quantified, another analysis was performed for the quantitative determination of these compounds.

The antioxidant activity of plant extracts was also investigated by DPPH radical scavenging assay and correlated with the total phenol content and total flavonoid content.

Experimental

Plant material and extraction procedure

The aerial parts of *A. annua*, *A. absinthium* and *A. vulgaris* were harvested at the flowering stage from the countryside around Iasi, Romania, in August-September 2014. The species were authenticated and a voucher specimen of each was deposited in the Herbarium of Pharmaceutical Botany Department from the Faculty of Pharmacy. The plants were air-dried at room temperature and grounded to a fine powder. 10 g of plant material was extracted three times with 200 mL methanol for 1 hour, at room temperature, using a magnetic stirrer. The extract was appropriately diluted before injection in HPLC.

Chromatographic conditions for the analysis of methoxylated flavones

Methoxylated flavonoid aglycones were quantified through high-performance liquid chromatography coupled with mass spectrometry (LC-MS), using six standards: jaceosidin, eupatilin (ALB Technology, China), casticin, acacetin, eupatorin, hispidulin (Sigma, Germany).

The separation of the methoxylated flavones was achieved using a Zorbax SB-C18 reversed-phase analytical column (100 × 3.0 mm i.d., 5 μm particle) fitted with a guard column Zorbax SB-C18, both operated at 48 °C. The mobile phase consisted of 0.1 % (v/v) acetic acid and methanol with the following gradient: beginning with 45 % methanol and ending at 50 % methanol, for 8 minutes with a flow rate of 0.9 mL min^{-1} and an injection volume of 5 μL. For the MS analysis the following optimized conditions were used: electrospray ionization (ESI) interface operating in negative mode, gas (nitrogen) temperature 325 °C at a flow rate of 12 L min^{-1}, nebulizer pressure 60 psi and capillary voltage -2500 V. The full identification of compounds was performed by comparing the retention times and mass spectra with those of standards in the same chromatographic conditions. The MS was operated in the multiple reactions monitoring analysis (MRM) mode instead of single ion monitoring.

Chromatographic conditions for the analysis of caffeic and chlorogenic acids

The two hydroxycynnamic acids (caffeic acid and chlorogenic acid from Sigma, Germany) were separated using a Zorbax SB-C18 reversed-phase analytical column (100 × 3.0 mm i.d., 3 μm particles) fitted with a guard column Zorbax SB-C18, both operated at 42 °C. The separation was achieved under isocratic conditions using a mobile phase consisting of 0.1 % acetic acid and acetonitrile (v/v). The flow rate was 0.8 mL min^{-1} and the injection volume was 5 μL. Mass spectrometry analysis was performed on an Agilent Ion Trap 1100 VL mass spectrometer with electrospray ionization (ESI) interface in negative mode. Operating conditions were optimized in order to achieve maximum sensitivity values: gas (nitrogen) temperature 60 °C at a flow rate of 12 L min^{-1}, nebulizer pressure 60 psi and capillary voltage - 3500 V. The full identification of compounds was performed by comparing the retention times and mass spectra with those of standards in the same chromatographic conditions. To avoid or limit the interference from background, the multiple reactions monitoring analysis mode was used instead of single ion monitoring (e.g., MS/MS instead of MS).

Determination of total flavonoid and total polyphenols content

The concentration of total phenols in plant extracts was estimated by Folin-Ciocalteu procedure.[8] 2 mL of the diluted samples were mixed with 10 mL of a Folin-Ciocalteu reagent dilution (1:10). After a period of time ranging between 30 seconds to 8 minutes, the Na_2CO_3 solution was added. The absorbance was determined after 2 h at 20 ºC, versus a zero-absorbance reagent blank. The blue color produced was measured at 760 nm using an Able Jasco V-550 UV-VIS spectrophotometer. The concentration of total phenolic compounds in extracts was calculated by comparison with a standard curve similarly prepared with 0 to 500 μg gallic acid 100 mL^{-1}. Total phenolic content values were determined using an equation that was obtained from the calibration curve of gallic acid graph (R^2=0.994). The total phenolic content of the sample was expressed as gallic acid equivalents which reflected the phenolic content as the amount of gallic acid (mg) in 1 g of dry material.

The flavonoids content in extracts was estimated by the spectrophotometric method described in Romanian Pharmacopoeia based on the reaction with aluminium chloride solution.[9] The 5 mL sample solution was placed in a 25 mL volumetric flask. Next, we added 5 mL solution of 100 g L^{-1} sodium acetate, followed by 3 mL of 25 g L^{-1} aluminium chloride solution in ethanol and the volume was made up with ethanol. After 15 minutes, the absorbance was determined at 350 nm versus a reagent blank. The flavonoids content in extracts was calculated by using quercetin (20-160 μg mL^{-1}) as a standard. The total flavonoids content values was determined using an equation obtained from the calibration curve of the quercetin graph (R^2 = 0.998). Results were expressed as mg equivalent quercetin per gram dry weight.

DPPH radical-scavenging activity

The free radical scavenging activity of the methanol extracts was measured in terms of hydrogen donating or radical scavenging ability using the stable DPPH radical method.[8] For this, the crude methanol extract was evaporated to dryness and dissolved in DMSO at different concentrations ranging from 0.3 to 10 mg mL^{-1}. 0.05 mL from each solution were added to 2.95 mL DPPH solution in methanol (A_{517nm} = 1.00 ± 0.05); the mixture was energetically shaken. After 5 minutes, the absorbance of the mixture was measured at λ = 517 nm. The percent DPPH scavenging ability (φ) was calculated using the formula:

$$\varphi = 100 \frac{A_{control} - A_{sample}}{A_{control}}$$

where

$A_{control}$ is the absorbance of methanol solution of DPPH radical (containing all reagents except the sample) and

A_{sample} is the absorbance of DPPH radical + sample extract, measured 5 minutes after the addition of extract.

Afterwards, a curve of % DPPH scavenging capacity *versus* concentration was plotted and EC_{50} values were calculated. EC_{50} denotes the concentration of sample required to scavenge 50% of DPPH free radicals. Quercetin was used as a positive control. All measurements were carried out in triplicate and results were expressed as mean value ± standard deviation.

Results and Discussion

The analysis of methoxylated flavones

Considering the fact that methoxylated flavones are bioactive compounds widely distributed in *Artemisia* genus, found generally as aglycones in the epicuticular wax, their determination is of interest from the point of view of utility of a medicinal plant. Thus, a new LC-MS method was developed in order to assess the presence of 6 methoxylated flavones in the plant extract i.e., jaceosidin, hispidulin, eupatilin, eupatorin, casticin and acacetin. The analytes eluted in less than 10 minutes in the chosen chromatographic conditions, as shown in Figure 1.

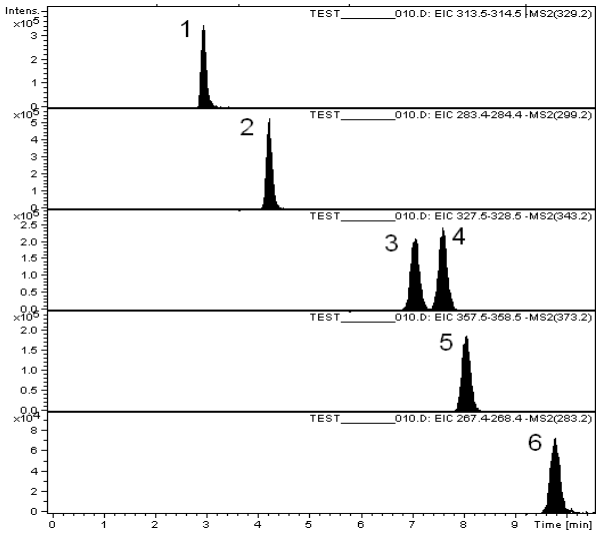

Figure 1. MS chromatograms of analyzed flavones: jaceosidin (1), hispidulin (2), eupalitin (3), eupatorin (4), casticin (5) and acacetin (6).

In the process of MS analysis, the pseudo-molecular ions of the flavones (329.3 for jaceosidin, 299.2 for hispidulin, 343.3 for eupatilin, 343.3 for eupatorin, 373.3 for casticin and 283.3 for acacetin) have been fragmented, and based on their daughter ions from the MS spectrum (Table 1) the extracted chromatograms of each compound were constructed for quantification. The calibration curves of methoxylated flavones were built and they all showed a linear correlation coefficient and a satisfactory level of precision and accuracy.

Table 1. Characteristic ions of standard flavones in full scan and specific ions used in quantification

Compound	R_T, min	M	$[M-H]^-$	Monitored ions/fragments
Jaceosidin	2.9	330.3	329.3	314
Hispidulin	4.2	300.2	299.2	284
Eupalitin	7.05	344.3	343.3	328
Eupatorin	7.6	344.3	343.3	328
Casticin	8.05	374.3	373.3	358
Acacetin	9.8	284.3	283.3	268

Table 2 shows the levels of methoxylated flavones found in the three medicinal plants analyzed.

It can be observed that all species contain casticin, hispidulin and eupatorin and lack jaceosidin and acacetin, although the two latter compounds are present in other *Artemisia* species.[10,11] Eupatilin is present only in *A. annua* in small amounts, while casticin is found in high concentrations in all three samples, most notably in *A. annua*.

Casticin is an active compound of *A. annua* that potentiate the antimalarial activity of artemisinin and exhibits modest antimicrobial activity against *Clostridium perfringens*.[12,13] Casticin also manifest antitumor activity against a large spectrum of cancer cell lines as well as anti-inflammatory activity.[14,15] A previous study lists casticin as one of three major components of *A. absinthium* plants cultivated in Spain, where it reaches a concentration (131 mg 1000 g^{-1} dw) similar to that found in our study.[16]

Hispidulin is a pharmacologically active flavone with anticancer and antiepileptic properties, while eupatorin has a broad spectrum of anticancer activity.[3,17] Eupatilin has potent anti-ulcer effect, strong anti-inflammatory and anti-oxidative activity and it is marketed in South Korea for the treatment of gastric inflammation in the form of standardized extract DA-9601.[18]

Flavones eupatorin and hispidulin were identified for the first time in *A. absinthium* and *A. vulgaris*. Also, the presence of eupatilin in *A. annua* and casticin in *A. vulgaris* is first reported in this study. Acacetin and jaceosidin were not identified in any of the three species, even though acacetin is mentioned in literature as a component of *A. annua*.[3]

Methoxylated flavonoids are promising therapeutic candidates due to their lipophilic nature and increased metabolic stability, that results in high oral bioavailability compared to other polyphenols.[19]

Caffeic and chlorogenic acids analysis

In the previous polyphenols analysis,[4] caffeic and chlorogenic acids - both powerful antioxidants, could not be quantified due to co-elution, so a new LC-MS method was used for their determination in plant extract.

In the aforementioned chromatographic conditions, the retention time of the chlorogenic was 2.2 minutes and of caffeic acid 3.3 minutes, as shown in Figure 2. Because in the ionization conditions both acids lose a proton, the ions monitored by the mass spectrometer are always in the form $[M-H]^-$, so the ions recorded have m/z = 353 for chlorogenic acid and m/z = 179 for caffeic acid. Further, in order to increase the selectivity and sensitivity of the method, for each compound, a second ion was monitored from the MS/MS spectrum: m/z 191 for chlorogenic acid and m/z 135 for caffeic acid.

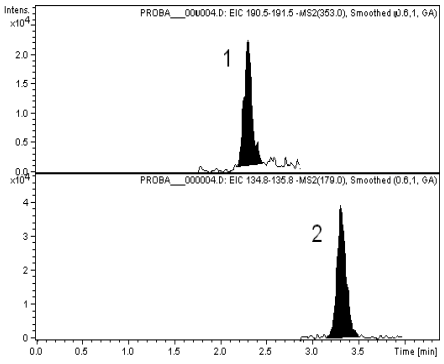

Figure 2. MS chromatograms of chlorogenic (1) and caffeic (2) acids

The ions with m/z = 191 and m/z = 135 were further used for the quantitative determination of these compounds, seeing that the intensity of ions in the mass spectrum is proportional to the concentration of the substance in the sample.

 DOI: 10.17628/ecb.2016.5.119-123

Table 2. Concentration of methoxylated flavones in plants

Plant	Concentration (μg g^{-1} dry weight plant material)			
	Eupatorin	**Eupatilin**	**Casticin**	**Hispidulin**
A. annua	21.86	2.98	1587.45	23.73
A. vulgaris	0.97	0.00	124.51	1.47
A. absinthium	36.24	0.00	199.10	15.01

Acacetin and jaceosidin were not found in any sample.

Table 3 presents the levels of caffeic and chlorogenic acids in the analyzed species. It can be noticed that chlorogenic acids predominates in all species, the highest concentrations of both the hydroxycinnamic acids were found in *A. annua* and *A. vulgaris* in comparable amounts.

Table 3. Concentration of caffeic and chlorogenic acids in plants

Plant	Concentration, μg g^{-1} dw plant material	
	Caffeic acid	**Chlorogenic acid**
A. annua	50.20	4658.60
A. vulgaris	23.20	3984.20
A. absinthium	11.80	1658.00

Another study found in Romanian *A. absinthium*, comparable amounts of caffeic acid (0.181 mg g^{-1} dry extract), but much lower levels of chlorogenic acid (0.077 mg g^{-1} dry extract) in the ethanol 70 % extracts of aerial parts.[20] The difference may arise from the different method of analysis and type of extract.

The methanol extract of *A. vulgaris* leaves collected from Serbia contains (0.44 mg g^{-1} dw) chlorogenic acid, almost ten times lower than our result, probably due to the difference in the analysis method.[21] An aqueous extract obtained from the aerial parts of *A. annua* cultivated in Italy was reported to contain 9.0 mg g^{-1} dw chlorogenic acid and 3.12 mg g^{-1} dw caffeic acid.[22] Again, the contrasting values may be explained through the variation of extract type, plant origin (cultivated versus wild) and distinct method of analysis.

Total phenols and total flavonoids content

The results are shown in Table 4. Both total flavonoid and total phenols content in plant extracts decreases in the following order: *A. annua* > *A. vulgaris* > *A. absinthium*.

Table 4. Total phenols and total flavonoids content in plants

Plant	Active ingredient content, mg g^{-1} dry weight plant material	
	Phenols	**Flavonoids**
A. annua	80.65	13.88
A. vulgaris	41.67	10.11
A. absinthium	18.14	3.23

Antioxidant activity

The radical scavenging activity (Table 5) of the extracts decreases in the following order *A. vulgaris* > *A. annua* > *A. absinthium*. The antioxidant activity of analyzed extracts is concentration dependent and is influenced by the level of phenolic compounds, but also by the nature of those compounds.

Table 5. Free radical (DPPH) scavenging activity of plants extracts

Plant	EC_{50} (μg mL^{-1})
A. annua	77.73 ± 1.15
A. vulgaris	41.3 ± 0.2
A. absinthium	88.83 ± 0.55

Other researchers reported EC_{50} values of 976 μg mL^{-1} of an ethanol 70 % extract from the whole *A. vulgaris* plant[23] or 16 μg mL^{-1} of a methanol extract from *A. vulgaris* leaves[21], the latter being closer to our result. Another study found a lower antioxidant activity of a methanol extract from *A. annua* leaves (EC_{50} = 190.54 μg mL^{-1}) compared to our results.[24] For *A. absinthium* extract in ethanol 70 %, Craciunescu et al. reported a powerful radical scavenging activity with EC_{50} = 0.57 μg mL^{-1}.[20]

Conclusions

Biologically active compounds were identified and quantified in three *Artemisia* species, commonly used in Romanian traditional medicine. Six methoxylated flavones and two hydroxycinnamic acids were analyzed through LC-MS methods. Occurrence of eupatorin and hispidulin in *A. absinthium* and *A. vulgaris*, eupatilin in *A. annua* and casticin in *A. vulgaris* are reported here for the first time

There was a significant difference in concentration between caffeic acid and chlorogenic acid, in favour of the last one. All extracts showed antioxidant effect, notably *A. vulgaris* extract which exhibited a very good scavenging activity against DPPH radicals. The plant species studied here are important sources of biologically active compounds that can be used for the treatment and prevention of diseases.

References

[1]Proksch, P., *Hagers Handbuch der Pharmazeutischen Praxis, Springer Verlag*, **1992**, 357.

[2]Bora, K. S., Sharma, A., *Pharm. Biol.*, **2011**, *49(1)*, 101.

[3]Ferreira, J. F. S., Luthria, D. L., Sasaki, T., Heyerick, A., *Molecules*, **2010**, *15*(*5)*, 3135.

[4]Ivanescu, B., Vlase, L., Corciova, A., Lazar, M. I., *Chem. Nat. Comp.*, **2010**, *46(3)*, 468.

[5]Yoon, K. D., Chin, Y. W., Yang, M. H., Kim, J., *Food Chem.*, **2011**, *129*, 679.

[6]Li, Y. J., Guo, Y., Yan, Y., Qing, Y., Weng, X. Z., Yang, L., Wang, Y. J., Chen, Y., Zhang, D., Li, Q., Liu, X. C., Kan, X. X., Chen, X., Zhu X. X., Kmoniekova, E., Zidek, Z., *Toxicol. Appl. Pharm*., **2015**, *286*(*3)*, 151.

[7]Estévez, S., Marrero, M. T., Quintana, J., Estévez, F., *PLoS One*, **2014**, *9(11)*, e112536.

[8]Zeidan, S., Hijazi, A., Rammal, H., Bazzal, A. A., Annan, A., Al-Rekaby, A., *Eur. Chem. Bull.*, **2015**, *4(11)*, 498.

[9]Romanian Pharmacopoeia Commission National Medicines Agency, *Romanian Pharmacopoeia, 10th edition, Medical Publishing Hous*e, **1993**.

[10]Al-Hazimi, H. M. G., Basha, R. M. Y., *J. Chem. Soc. Pak.*, **1991**, *13(4)*, 277.

[11]Suleimen, E. M., Dzhalmakhanbetova, R. I., Ishmuratova, M. Y., *Chem. Nat. Comp.*, **2014**, *50(5)*, 918.

[12]Elford, B. C., Roberts, M. F., Phillipson, J. D., Wilson, R. J., *Trans. R. Soc. Trop. Med. Hyg*., **1987**, *81*, 434.

[13]Ivarsen, E., Fretté, X. C., Christensen, K. B., Christensen, L. P., Engberg, R. M., Grevsen, K., Kjaer, A., *J. AOAC Int.*, **2014**, *97(5)*, 1282.

[14]Rasul, A., Zhao, B. J., Liu, J., Liu, B., Sun, J. X., Li, J., Li, X. M., *Asian Pac. J. Cancer. Prev.*, **2014**, *15(21)*, 9044.

[15]Li, Y. J., Guo, Y., Yang, Q., Weng, X. G., Yang, L., Wang, Y. J., *Toxicol. Appl. Pharm.*, **2015**, *286*, 151.

[16]Gonzalez-Coloma, A., Bailen, M., Diaz, C. E., Fraga, B. M., Martínez-Díaz, R., Zuñiga, G. E., Contreras, R. A., Cabrera, R., Burillo, J., *Ind. Crop. Prod.*, **2012**, *37*, 401.

[17]Atif, M., Ali, I., Hussain, A., Hyder, S. V., Niaz, B., Khan, F. A., Maalik, A., Farooq, U., *Acta Pol. Pharm.*, **2015**, *72(5)*, 829.

[18]Ryoo, S. B., Oh, H. K., Moon, S. H., Choe, E. K., Oh, T. Y., Park, K. J., *Korean J. Physiol. Pharmacol.*, **2014**, *18*, 383.

[19]Walle, T., *Semin. Cancer Biol.*, **2007**, *17(5)*, 354.

[20]Craciunescu, O., Constantin, D., Gaspar, A., Toma, L., Utoiu, E., Moldovan, L., *Chem. Cent. J.*, **2012**, *6(1)*, 97.

[21]Melguizo-Melguizo, D., Diaz-de-Cerio, E., Quirantes-Piné, R., Švarc-Gajić, J., Segura-Carretero, A., *J. Funct. Foods*, **2014**, *10*, 192.

[22]D'Abbaddo, T., Carbonara, T., Argentieri, M. P., Radicci, V., Leonetti, P., Villanova, L., Avato, P., *Eur. J. Plant. Pathol.*, **2013**, *137*, 295.

[23]Oyedemi, S. O., Coopoosamy, R. M., *Int. J. Pharmacol.*, **2015**, *11(6)*, 561.

[24]Lee, J. H., Lee, J. M., Lee, S. H., Kim, Y. G., Lee, S., Kim, S. M., Cha, S. W., *Hortic. Environ. Biotechnol.*, **2015**, *56(5)*, 69.

Received: 03.04.2016.
Accepted: 21.05.2016.

S- LINE AND ENTROPY IN TECHNOLOGY, ECONOMICS AND PHYSICO-CHEMICAL STUDIES

G. A. Korablev,[a]* G. E. Zaikov,[c] V. I. Kodolov,[b] Yu. G. Vasiliev,[a] P. L. Maksimov,[a] N. G. Petrova[d] and P. B. Akmarov[a]

Keywords: Entropy, nomogram, spatial-energy parameter, biophysical processes, business, engineering systems.

The concept of the entropy of spatial-energy interactions is used similarly to the ideas of thermodynamics on the static entropy. In this research we are trying to apply the concept of entropy to assess the degree of spatial-energy interactions using their graphic dependence and a nomogram to assess the entropy of different processes is obtained. The variability of entropy demonstrations is discussed, in biochemical processes, economics and engineering systems as well.

* Corresponding Authors
E-Mail: korablevga@mail.ru
[a] Department of Physics, Izhevsk State Agricultural Academy, Russia.
[b] Department of Chemistry and Chemical Engineering of Kalashnikov Izhevsk State Technical University, 426069, Izhevsk, Studencheskaya 7, Russia.
[c] Institute of Biochemical Physics, Russian Academy of Science, Russia.
[d] Agency of Informatization and Communication, Udmurt Republic

Introduction

In statistical thermodynamics, the entropy of the closed and equilibrious system equals the logarithm of the probability of its definite macrostate (Eqn.1).

$$S = k \ln W \qquad (1)$$

where

W is the number of available states of the system or degree of the degradation of microstates and

k is Boltzmann's constant.

or

$$W = e^{s/k} \qquad (2)$$

These correlations are general assertions of macroscopic character, they do not contain any references to the structure elements of the systems considered and they are completely independent of microscopic models.[1] Therefore the application and consideration of these laws can result in a large number of consequences.

At the same time, the main characteristic of the process is the thermodynamic probability *W*. In actual processes of the isolated-system type, the entropy growth is inevitable i.e., disorder and chaos increase in the system the quantity of internal energy goes down. The thermodynamic probability equals the number of microstates corresponding to the given macrostate. Since the degree of system degradation is not connected with the physical features of the systems, the entropy statistic concept can also have other applications and demonstrations, apart from statistical thermodynamics.

It is clear that in two systems, completely different in their physical content, the entropy can be the same if their number of possible microstates corresponding to one macroparameter (whatever parameter it is) coincides. Therefore the idea of entropy can be used in various fields. The increasing self-organization of human society leads to the increase in entropy and disorder in the environment that is demonstrated, in particular, by a large number of disposal sites all over the earth.[2]

In this article, we are trying to apply the concept of entropy to assess the degree of spatial-energy interactions using their graphic dependence, and in other fields.

Entropic nomogram of the degree of spatial-energy interactions

The idea of spatial-energy parameter (*P*-parameter), which is the complex characteristic of the most important atomic values responsible for interatomic interactions and having the direct bond with the atom electron density, was introduced based on the modified Lagrangian equation for the relative motion of two interacting material points.[3] The value of the relative difference of *P*-parameters of interacting atoms-components – the structural interaction coefficient α is used as the main numerical characteristic of structural interactions in condensed media (Eqn. 3).

$$\alpha = \frac{P_1 - P_2}{(P_1 + P_2)/2} * 100 \qquad (3)$$

Applying the reliable experimental data, we obtained the nomogram of structural interaction degree dependence (ρ) on coefficient α, for a wide range of structures (Figure 1).

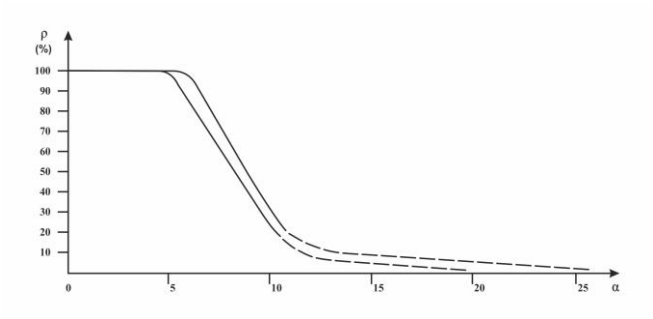

Figure 1. Nomogram of dependence of degree of structural interactions (ρ) on coefficient α.

This approach raises a possibility of evaluating the degree and direction of the structural interactions of phase formation, isomorphism and solubility processes in multiple systems, including molecular ones. Such nomogram can be demonstrated[3] as a logarithmic dependence also (Eqn. 4).

$$\alpha = \beta\left(\ln \rho\right)^{-1} \qquad (4)$$

where coefficient β is the constant value for the given class of structures. β can structurally change mainly within ± 5% from the average value. Thus coefficient α is inversely proportional to the logarithm of the degree of structural interactions and therefore can be characterized as the entropy of spatial-energy interactions of atomic-molecular structures.

Actually the more is ρ, higher is the probability of the formation of stable ordered structures (e.g. the formation of solid solutions), i.e. the less is the process entropy and also the less is coefficient α. The equation (4) does not have the complete analogy with Boltzmann's equation (1) as in this case not the absolute but only relative values of the corresponding characteristics of the interacting structures are compared which can be expressed in percent. This refers not only to coefficient α but also to the comparative evaluation of structural interaction degree (ρ), for example, the percent of atom content of the given element in the solid solution relatively to the total number of atoms. Therefore in equation (4) coefficient k = 1. Thus, the relative difference of spatial-energy parameters of the interacting structures can be a quantitative characteristic of the interaction entropy, i.e. α≡*S*.

Entropic nomogram of surface-diffusive processes

As an example, let us consider the process of carbonization and formation of nanostructures during the interactions in polyvinyl alcohol gels and copper oxides or chlorides. At the first stage, small clusters of inorganic phase are formed surrounded by carbon containing phase. In this period, the main character of atomic-molecular interactions needs to be assessed via the relative difference of *P*-parameters calculated by involving the radii of copper ions and covalent radii of carbon atoms. In the next main carbonization period the metal phase is being formed on the surface of the polymeric structures. From this point, the binary matrix of the nanosystem, C → Cu, is being formed.

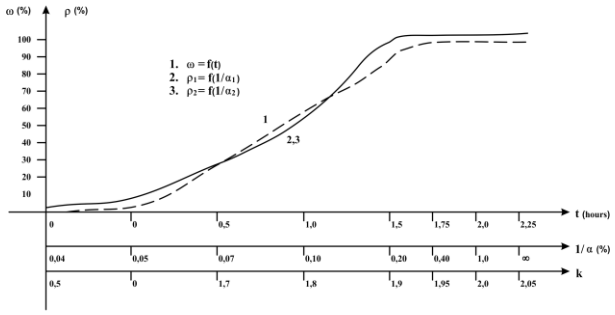

Figure 2. Dependence of the carbonation rate coefficient α in the formation of nanosystems C→Cu

The values of the degree of structural interactions, calculated from coefficient α by Eqn. 5, are given in Figure 2 (curve 2). Here, the graphical dependence of the degree of nanofilm formation (ω) on the process time is presented by the data obtained earlier[4] (curve 1) and previously obtained nomogram from Eqn. 6 is presented in curve 3.

$$\rho_1 = f\left(\frac{1}{\alpha_1}\right) \qquad (5)$$

$$\rho_2 = f\left(\frac{1}{\alpha_2}\right) \qquad (6)$$

The analysis of all the observed graphical dependencies demonstrates the practically complete graphical coincidence of all the three graphs with slight deviations in the beginning and end of the process. Thus, the carbonization rate, as well as the functions of many other physical-chemical structural interactions, can be accessed from the values of the calculated coefficient α and entropic nomogram.

Entropy in the kinetics of physiological processes

The formation of ferment-substrate complex is the necessary stage of fermentative catalysis. One or more than one substrate molecules can join the ferment molecule.[5] For ferments with stoichiometric coefficient not equal one, the type of graphical dependence of the reaction product performance rate (μ) depending on the substrate concentration (c) has a sigmoid character with the specific bending point (Figure 3).[6] From Figure 3 it is apparent that this curve in general is similar to the character of the entropic nomogram in Figure 1. The graph of the dependence of electron transport rate in biostructures on the diffusion time scale of ions is similar.[6]

In the procedure of assessing fermentative interactions, it was assumed that the effective number of interacting molecules is more than one. In the methodology of ρ-parameter, a ferment has a limited isomorphic similarity with substrate molecules and does not form a stable compound with them, but, at the same time, some limited reconstruction of chemical bonds takes place, which makes it possible to obtain the final product.

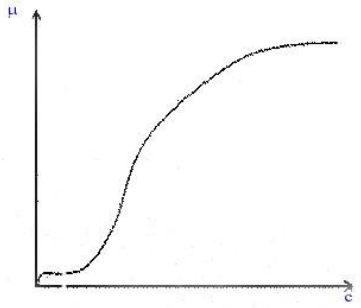

Figure 3. Dependence of the fermentation reaction rate (μ) on the substrate concentration (*c*)

Dependence of biophysical criteria on their frequency characteristics

The passing of alternating current through live tissues is characterized by the dispersive curve of electrical conductivity, which is directly dependent on the total resistance of tissue (*z*-impedance) on the alternating current frequency logarithm (log ω). Normally, such curve, on which the impedance is plotted on the coordinate axis, and log ω on the abscissa axis, formally, completely corresponds to the entropic nomogram (Figure 1). The fluctuations of biomembrane conductivity (conditioned by random processes) have the form of Lorentz curve.[5] In this graph, the fluctuation spectral density (ρ) is plotted on the coordinate axis, and the frequency logarithm function (log ω) on the abscissa axis. The type of such curve also corresponds to the entropic nomogram in Figure 1.

Lorentz curve of spatial-time dependence

In Lorentz curve[7] the space-time graphic dependence (Figure 4) of the velocity parameter (θ) on the velocity itself (β) is given, which completely corresponds to the entropic nomogram given in Figure 1.

Entropic criteria in economic processes

The concept of thermodynamic probability as a number of microstates corresponding to the given macrostate can be modified as applicable to the processes of economic interactions that directly depend on the parameters of business structures. Thus it is supposed that such number of workers of the business structure is the analog of thermodynamic probability as applicable to the processes of economic interactions in business. It can be accepted that the total entropy of a business enterprise consists of two entities characterizing a decrease in the competition efficiency (S_1) and a decrease in the personal interest of each worker (S_2), i.e. $S = S_1 + S_2$. S_1 is proportional to the number of workers in the company, $S \propto N$, and S_2 has a complex dependence not only on the number of workers in the company but also on the efficiency of its management.

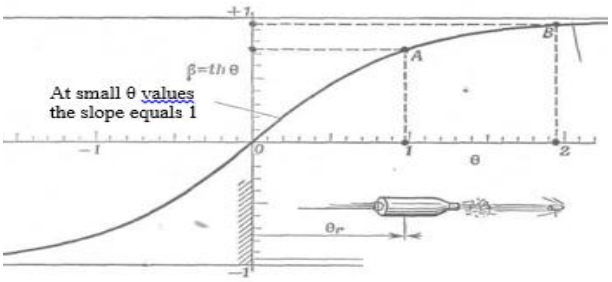

Figure 4. Connection between the velocity parameter (Θ) and velocity itself (β=thΘ)

It is inversely proportional to the personal interest of each worker. Therefore it can be accepted that $S_2 = 1/\gamma$, where γ is the coefficient of personal interest of each worker.

By analogy with Boltzmann's eqn. 1, we have

$$S = \ln\left(\frac{N}{\gamma}\right) \qquad (7)$$

In Table 1 one can see the approximate calculations of business entropy by Eqn. 7, for three main levels of business, small, medium and large. At the same time, it is supposed that number *N* corresponds to some average value of the most probable values. When calculating the coefficient of personal interest, it is considered that it can change from 1 (one self-employed worker) to zero (0), if such worker is a deprived slave, and for larger companies it is accepted that γ = 0.1 – 0.01.

Despite the rather approximate accuracy of such averaged calculations, we can make a resonably reliable conclusion of the fact that business entropy, with the aggregation of its structures, sharply increases during the transition from the medium to large business as the quality of business processes decreases.

Table 1. Entropy growth with an increase in business increase.

Structural parameter	Business Size		
	Small	**Medium**	**Large**
$N_1 – N_2$	10 – 50	100 – 1000	10000 – 100000
γ	0.9 – 0.8	0.6 – 0.4	0.1 – 0.01
S	2.408–4.135	5.116–7.824	11.513 – 16.118
<*S*>	3.271	6.470	13.816

Comparing the nomogram of Figure 1 with the data from the Table 1, we can see the additivity of business entropy values (*S*) with the values of the coefficient of spatial-energy interactions (á), i.e. $S = \alpha$.

S-curves

Some general regularities of the development in biological systems (growth in the number of bacteria colonies, population of insects, weight of the developing fetus, etc.) have been found even in the last century.[8] The curves reflecting these growths were similar. First of all, there are three successive stages, slow increase, fast burst-type growth and stabilization (sometimes decrease).

The engineering systems go through similar stages during their development. The curves drawn up in coordinate system where the numerical values of the important operational characteristics (for example, aircraft speed, electric generator power, etc.) were showed on the vertical and the age of the engineering system/costs of its development was showed on the horizontal axe were called S-curves (by the curve appearance). These curves are sometimes also called life lines. As an example, a graph of the changes in steel specific strength with time (by years) is shown (Figure 5).[8]

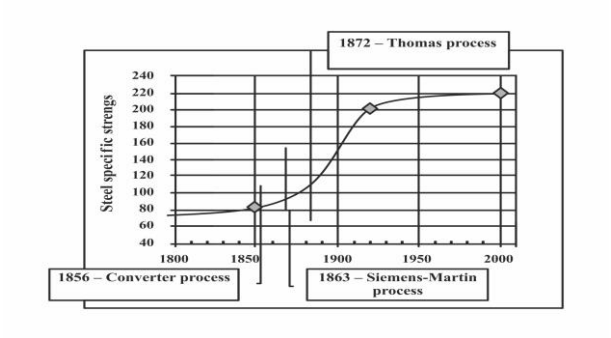

Figure 5. Dependence of steel specific strength on time

Thus, the similarity between *S*-curves and entropic nomogram in Figure 1 is apparent. The time dependence (*t*) is proportional to the reverse of entropy reverse ($1/\alpha$). As applicable to business, such curves characterize the process intensity, for example, sale of the given products. At the same time, entropic nomograms in accordance with Figure 1 assess the business quality (ordinate in such graphs).

Entropic processes in physiological systems

The resources often are closed without exhausting in the real processes when the system starts a more effective similar function and attracts the resources to itself (Figure 6).[8] This is characteristic not only for the short-term processes but also for general development of interstructural and cellular interactions.

It is much more complicated to consider and mathematically analyze the heteromorphic and rather dynamic intercellular and cellular-cellular interactions during ontogenesis. Nevertheless it is possible to reveal some regularities of such energy-molecular and -macromolecular interactions even at early stages of embryogenesis. In particular, relatively stable cellular- cellular interconnections are revealed which can alternate with the manifestations of instability with the activation of cell immigration to the areas of their definitive location.

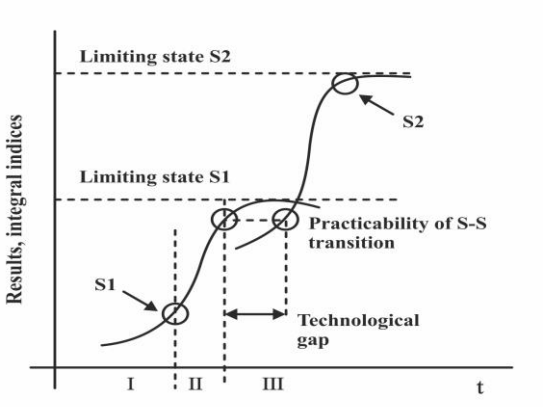

Figure 6. Entropic transitions by time *t*

As examples, stable focal cellular-cellular interconnections in the areas of simple contacts and desmosomes are often based on similar glycoprotein and lipoprotein macromolecular interactions with opposite interaction poles. At the same time, rather unstable selectin and integrin bonds differ in heteromorphism of cellular-cellular bonds or compounds of the proteins indicated with intercellular matrix that increases the instability of such bonds.

The heterotypicity of organization of peptide-peptide and other focal cellular-cellular interactions is more probably accompanied by the manifestation of energetically unstable bonds enhancing the irregularity of biological systems. This, in turn, contributes to forming dynamic and rather unstable compounds facilitating the cell migration and other manifestations of cellular instability. It is the increase in structural diversity, and thus controllable transitory enhancement of the system chaotic character, that can be the basis starting up the transition to new states, to the development individual cells, cell populations in general (in accordance with Figure 6).[9]

It is obvious that, in general, self-organizing processes follow the same principle i.e. slow development from structural diversity, fast growth and stabilization of the renewed biosystem. Thus, the nature fights with entropy development in the organism maintaining it at the constant level as the main condition of stationary state.

Conclusion

As it is known the entropy of isolated systems does not decrease. In open systems the entropy growth is compensated by the negative entropy due to the interaction with the environment.

All the systems discussed above can be considered as open ones. This also refers to spatial-energy processes at which any change in dimensional energy characteristics is conditioned by interactions with external systems. The same is apparently observed in connection with technical and technological systems, in whose development dynamics the additional innovations, modifications and financial investments take place.

The entropy in thermodynamics is considered as the measure of irreversible energy dissipation. From the position of technological and economic principles, entropy is essentially the measure of irrational consumption of energy resources. With the increase in time dependence, such processes stabilize in accordance with nomograms to the most optimal values, together with anti-entropy growth, i.e. the value of $1/\alpha = 1/S$.

The similar growth with time of rationality of technological, economic, and physical and mathematical parameters indicates that their nomograms are universal for the majority of main processes in nature, technology and economics.

Finally, it can be concluded that the idea of entropy is diversified in physical and chemical, economic, engineering and other natural processes which is confirmed by their nomograms.

References

[1]Reif, F., *Statistic Physics*, Nauka, Moscow, **1972**, 352.

[2]Gribov, L. A., Prokofyeva, N. I., *Basics of Physics*, Ì.: Vysshaya shkola, Moscow, **1992**, 430.

[3]Korablev G. A., *Spatial-Energy Principles of Complex Structures Formation*, Brill Academic Publishers, Leiden, **2005**, 426.

[4]Kodolov, V. I., Khokhriakov, N. V., Trineeva, V. V., Blagodatskikh, I. I., *Chem. Phys. Mesoscopy*, **2008**, *10*, 448-460.

[5]Rubin, A.B., *Biophysics Book 2, Biophysics of Cell Processes*, Vysshaya shkola, Moscow, **1987**, 319.

[6]Rubin, A. B., *Biophysics Book 1, Theoretical Biophysics*, Vysshaya Shkola, Moscow, **1987**, 319.

[7]Taylor, E., J. Wheeler, J., *Spacetime Physics*, Mir Publications, Moscow, 1**987**, 320.

[8]Kynin, À. Ò., Lenyashin, V. A., *Assessment of the parameters of engineering systems using the growth curves*, http://www.metodolog.ru/01428/01428.html

[9]Lyubomirsky A., Litvin S. *Laws of engineering system development /* *http://www.metodolog.ru/00767/00767.html*

Received: 24.05.2016.
Accepted: 12.05.2016.

PREDICTION OF PREDOMINANT CONFIGURATION IN THE ENANTIOSELECTIVE REDUCTION OF β-KETOACID DERIVATES WITH BAKER'S YEAST USING NEURAL NETWORKS

Didier Villemin,[a]* Driss Cherqaoui[a] and Abdelhalim Mesbah[b]

Keywords: β-ketoacid; reduction; enantioselectivity; prediction; neural networks.

Correlation between chemical structure and enantioselectivity in baker's yeast reduction of a set of carbonyl compounds was constructed by means of a multi-layer neural network using the back-propagation algorithm. To evaluate the predictive power of the neural network (NN) model, the cross-validation procedure was used, 88 % of the reactions were correctly predicted.

* Corresponding Authors
E-Mail: villemin@ensicaen.fr
[a] Normandie Université, France, ENSICAEN, LCMT, UMR CNRS 6507, INC3M, FR 3038, Labex EMC3, Labex SynOrg, 14050 Caen, France.
[b] University Cadi Ayyad, Faculty of Sciences, Depart. Chemistry, BP 2390, Marrakech, Marocco.

Introduction

Concerning the enantioselective reduction of carbonylated compounds, the prediction of the preferred alcohol enantiomer in synthesis is a difficult task. For the prediction of the R/S configuration in an asymmetric reduction of carbonyl compounds, Prelog, Cram and Felkin have developed models of limited applicability based on steric criteria.[1]

J. Aires de Sousa *et al* have studied the enantioselective reduction of ketones by DIP-chloride,[2] the addition of diethylzinc on benzaldehyde[2] and the enantioselective hydrolysis of ester by *Pseudomonas*,[3] all predictions were made using neural network. Using also neural networks for prediction of enantioselectivity, W. M. F. Fabian *et al* [4] have described the ring opening of epoxide by hydrolases.

In our study, the baker's yeast (*Saccharomyces cerevisiae*) enantioselective reduction of β-ketoacid derivates was chosen because of its importance in preparation of chiral alcohols (Fig. 1). Numerous enzymatic systems which are present, can perform such a reduction, but different experimental conditions do not generally influence the resulted configuration.[5]

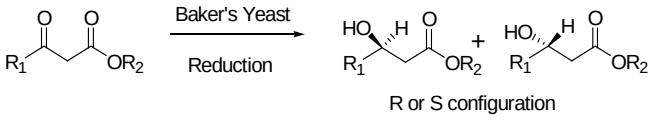

Figure 1. Bakers' yeast reduction of β-ketoacid derivates

Neural Networks (NNs) have successfully been used in organic chemistry,[7] particularly in QSAR studies, where numerous enzymatic systems and metabolic ways are implicated.[8] NNs are mathematical models of biological neural systems which fit non-linear problems and give better correlations than the multiple linear regression (MLR) ones. A description of the back-propagation algorithm was given previously[9] as well a more extensive description.[7] An attempt of structure-enantioselectivity relationships using neural networks was already described,[10] but the authors were unable to make predictions with molecular refraction[22] and finally proposed a Prelog model.

Methods

For our study, 35 reactions were extracted from reviews by Servi and Czuk et al.[6], where we can find the nearby experimental conditions (Table 1). Under these reactions the enantioselectivity was generally total, therefore our attention was focused on the prediction of R/S configuration of the produced enantiomer.

Previous studies[3,11] have shown that the correlation between the structure of the starting ketone and the alcohol obtained depends on steric criteria but other effects can also occur such as electronic ones. Therefore, the substituting groups R_1 and R_2 can be described by 2 kinds of parameters, electronic and steric parameters.

Electronic parameters: Hammett[12] assigned to every substituent a constant σ which represents its electronic effects on the reaction site. Taft *et al.*[13] have suggested two models where inductive and resonance contributions are quantitatively separated.

Steric parameters: Several studies[16] could be found in literature concerning the steric effects of substituent groups in organic reactions.[17]

Table 1: Chemical structures of the compounds studied

No	R_1	R_2	No	R_1	R_2	No	R_1	R_2
1	CH_3	C_2H_5	13	C_2H_5	C_8H_{17}	25	$CH_2CH_2CH=CH_2$	tC_4H_9
2	CH_3	nC_3H_7	14	NC_3H_7	C_8H_{17}	26	$CH_2CH_2C(CH_3)=CH_2$	CH_3
3	CH_3	nC_5H_{11}	15	NC_4H_9	C_2H_5	27	$CH_2CH_2C(CH_3)=CH_2$	C_2H_5
4	CH_3	nC_8H_{17}	16	CH_2Cl	CH_3	28	$CH_2CH_2CH=CH_2$	H
5	CH_3	iC_3H_7	17	CH_2Cl	C_2H_5	29	$CH_2CH_2CH=CH_2$	CH_3
6	CH_3	Ph	18	CH_2Br	C_2H_5	30	$CH_2CH_2CH=CH_2$	C_2H_5
7	CH_3	CH_3	19	CH_2Br	nC_3H_7	31	CH_2Cl	nC_8H_{17}
8	CH_3	nC_4H_9	20	CH_2Br	nC_7H_{15}	32	C_2H_5	nC_8H_{17}
	CH_3							
9	CH_3	tC_4H_9	21	CH_2Br	nC_8H_{17}	33	NC_3H_7	H
10		CH_3	22	CCl_3	C_2H_5	34	NC_3H_7	C_2H_5
11	C_2H_5	C_2H_5	23	CF_3	C_2H_5	35	NC_4H_9	H
12	Ph	C_2H_5	24	CH_3	C_2H_5			

Hansch *et al.*[18] proposed molecular refraction and molecular mass as sample measures of steric effects of substituting groups. In this latter study, the steric parameter is the volume of the substituents (V) computed using the Gavezzotti method.[19]

Results and discussions

A three layers Neural Network (NN) was used with the back-propagation (BP) algorithm for the prediction of predominant configuration (R or S) of the final product. Two methods were used to describe the reactions:

First method: Every reaction is described by 6 parameters σ_m, σ_p and V for R_1 and the same for R_2, this represents the input layer (6 neurons). The output layer contains only one neuron, which takes the value of 1 if the predominant configuration is S and 0 if it is R.

Second method: In this case, four parameters were used to describe each substituent (σ_m, σ_p, *V* and *L*), where *L* is the Verloop[20] parameter *L* represents the length of the substituent along the bond axis between the substituent atom and the parent compound, it was chosen because it permits to distinguish isomers.

We used a network with 6 or 8 units and a bias in the input layer, a variable hidden layer including bias, and one unit in the output layer. Input and output data were normalized between 0.1 and 0.9. The weights were initialized to random values between -0.5 and +0.5 and no momentum was added. The learning rate was initially set to 1 and was gradually decreased until the error function could no longer be minimized. All computations were performed using our own programs, written in the C language.

Learning. In order to determine the best architecture, different NNs have been tried using the two description systems [6-*x*-1 and 8-*x*-1; *x* = 1, 2, 3, 4, 5, 6, ...) with the all 35 reactions as a training set. The criteria used for the comparison of the architectures is the percentage of reactions correctly classified. We consider that we have a correct classification for a reaction if the output neuron was greater than 0.6 for S configuration and less than 0.4 for R configuration. After 2000 iterations, the NNs of structure [6-*x*-1] (*x*=2,3,4,5) were able to classify 34 of the 35 reactions studied.

Prediction. The predictive ability of an NN is its ability to give a satisfactory output for a molecule not included in the examples the NN learned. To determine that predictive ability, cross-validation has been used.[21] After 1400 iterations in the cross validation procedure, 29 of the 35 reactions were correctly predicted (Table 3) with an NN [6-3-1] and [6-4-1] and 31 reactions of the 35 reactions (88 %) are correctly predicted with an NN (8-3-1). Clearly the parameter L provides new information to the NN.[22] The use of percent (% of S) or 2 neurons (0,1) as output does not improve the results.

We have used σ_m and σ_p parameters introduced by Taft for electronic effects of meta and para positions. These parameters are available in the literature[14] and Kvasnicka has shown[15] that these parameters can be computed by a neural network using simple structural data as inputs.

Table 2. Prediction results using the first method

NN architecture	Number of reactions correctly predicted/35
6-1-1	26
6-2-1	27
6-3-1	29
6-4-1	29

Table 3. Prediction results using the second method

NN architecture	Number of reactions correctly predicted/35
8-1-1	26
8-2-1	30
8-3-1	31
8-4-1	30

Conclusion

After the neural network has been fully trained, it has shown that the network was able to form reliable generalizations to predict R/S configuration in baker's yeast reduction of the carbonyl compounds presented to it. This shows that steric and electronic parameters (σ_m, σ_p, *V* and *L*) provide sufficient information to a neural network for prediction of the reactivity of the compounds studied. This study represents a first approach to the prediction of enatioselectivity, the efficiency of induction depends on the concentrations of substrats, and for a quantitative prediction this factor must be added to steric and electronic parameters.

Acknowledgments:

We thank Dr. J.M. Cense (Chimie ParisTech) for computation of the volumes.

References and notes

[1](a)Cram, D. J., Abd Elhafez, F. A., *J. Am. Chem. Soc*., **1952**, *74*, 5828-5835; (b) Chérest, M., Felkin, H., Prudent, N., *Tetrahedron Lett.*, **1968**, 2199-2204; (c) Prelog, V., *Pure Appl. Chem*., **1964**, *9*, 119-130.

[2]Joao Aires-de-Sousa, J., Gasteiger, J., *J. Chem. Inf. Comput. Sci*., **2001,** *41*, 369-375

[3]Zhang, Q. Y., Aires-de-Sousa, J., *J. Chem. Inf. Model.*, **2006**, *46*, 2278-2287

[4]Funar-Timofei, S., Suzuki, T., Paier, J. A. , Steinreiber, A., Faber, K., Fabian, W. M. F., *J. Chem. Inf. Comput. Sci.*, **2003,** *43*, 934-940

[5]Zhou, B., Gopalan, A. S., Van Middelsworth, F., Shieh, W., Sih, C. J., *J. Am. Chem. Soc*., **1983**, *105*, 5925-5928.

[6](a)Servi, S., *Synthesis*, **1991**, 1-25; (b) Csuk, R., Glänzer, B. I., *Chem. Rev*., **1991**, *91*, 49-97; (c) Santaniello, E., Ferraboschi, P., Grisenti P., Manzocchi, A., *Chem. Rev*., **1992**, *92*, 1071-1140; (d) Theil, F., *Chem. Rev*., **1995**, *95*, 2203-2227; (e) Hall, M., Bommarius, A. S., *Chem. Rev*., **2011**, *111*, 4088-4110; (f) Strohmeier, G. A., Pichler, H., May, O., Gruber-Khadjawi, M., *Chem. Rev.*, **2011**, *111*, 4141-4164.

[7](a)Zupan, J., Gasteiger, J., *Neural Networks for Chemists, An Introduction*, VCH editor, New York, **1993**; (b) Zupan, J., Gasteiger, J., *Neural Networks in Chemistry and Drug Design: An Introduction*, 2nd Edition**,** Wiley editor, **1999**; ISBN: 978-3-527-29779-5.

[8](a)Andrea. T. A., Kalayeh, H., *J. Med. Chem.* **1991**, *34*, 2824-2836; (b)So, S. S., Richards, W. G., *J. Med. Chem*. **1992**, *35*, 3201-7; (c) Villemin, D., Cherqaoui D., Cense, J. M., *J. Chim. Phys.*, **1993**, *90*, 1505-1519; (d)Ajay, A., *J. Med. Chem.*, **1993**, *36*, 3565-3571.

[9]Cherqaoui, D., Villemin, D., *J. Chem. Soc. Faraday Trans.*, **1994**, *90*, 97-102.

[10]Zakarya, D., Farhaoui, L., Fikh-Tetouani, S., *Tetrahedron Lett.*, **1994**, *35*, 4985- 4988.

[11]Shieh, W., Gopalan, A. S., Sih, C. J., *J. Am. Chem. Soc.*, **1985**, *107*, 2993-2994.

[12](a)Hammett. L. P., *J. Am. Chem. Soc.*, **1937**, *59*, 96-103; (b) Hammett. L. P., *Physical Organic Chemistry*, 2nd edition, McGraw-Hill, New York, **1970**.

[13](a)Taft, R. W., Lewis, I. C., *J. Am. Chem. Soc*., **1958**, *80*, 2436-2436; (b) Taft, R. W., Lewis, I. C., *J. Am. Chem. Soc.*, **1959**, *81*, 5343-5352.

[14]Hansch, C., Leo, A., *Substituent Constants for Correlation Analysis in Chemistry and Biology*, John Wiley editor, New York, **1979**.

[15]Kvasnicka, V., Sklenak, S., Pospichal, J., *J. Am. Chem. Soc.*, **1993**, *115*, 1495-1500.

[16](a)Taft, R. W., Newman, M. S., *Steric Effects in Organic Chemistry*, John Wiley editor, New York, **1956**, 556-565; (b) Charton, M., *Prog. Phys. Org. Chem.*, **1989**, *13*, 119-251; (c) Gallo, R. *Prog. Phys. Org. Chem.*, **1983**, *14*, 115-163; (d) Kutter, E., Hansch, C., *J. Med. Chem.*, **1969**, *12*, 647-652.

[17]Unger, S. H., Hansch, C., *Prog. Phys. Org. Chem.*, **1976**, *12*, 91-118.

[18]Hansch, C., Leo, A., Unger, S. H., Kim, K. H., Nikaitani, D., Lien, E. J., *J. Med. Chem.*, **1973**, *16*, 1207-1216.

[19]Gavezzotti, A., *J. Am. Chem. Soc.*, **1983**, *105*, 5220-5225.

[20]Verloop, A., Hoogenstraaten, W., Tipker, J., *Drug Design*, **1976**, *7*, 165-207.

[21]Cherqaoui, D., Villemin, D., Mesbah, A., Cense, J. M., Kvasnicka, V., *J. Chem. Soc. Faraday Trans*, **1994**, 90, 2015-2019.

[22]For example:[L(n-Pr) = 5.05 Å and L(iPr) = 4.11 Å], contrary to volume (V) and molecular refraction (MR) which indicates only the bulk [V(nPr) = 60.67Å^3 and V(iPr) = 60.63Å^3 ; MR(nPr) = MR(iPr)].

Received: 31.03.2016.
Accepted: 06.06.2016.

SYNTHESIS, STRUCTURAL CHARACTERIZATION AND BIOLOGICAL APPLICATION OF MIXED LIGANDS COMPLEXES OF COUMARIC ACID AND COUMARINE WITH SOME TRANSITION METAL CATIONS

Sineray Koç,[a] Dursun Ali Köse[a]* and Emre Avci[b]

Keywords: Biological activity, coumarin, mixed ligand, coumaric acid, metal complexes, spectroscopic methods.

Four new mixed ligand transition metal (Co(II), Ni(II), Cu(II) and Zn(II)) complexes of *p*-coumaric acid and coumarine have been synthesized and the structurally characterized. These complexes contain hydrate water except the Cu(II) complex. Coumaric acid is a monodendate ligand except Cu(II)-complex in which a bidendate coordination mode could be observed. The thermal decomposition starts with dehydration of Co(II), Ni(II) and Zn(II) complexes while in Cu(II) complex decomposition starts with fragmentation of organic ligands at 145 °C. Studies on their biological activity have also been performed. Molecular formulas of the obtained complex are as follows: (**I**) $[Co(C_9H_7O_3)_2(C_9H_6O_2)_2(H_2O)_2]\cdot 4H_2O$; (**II**) $[Ni(C_9H_7O_3)_2(C_9H_6O_2)_2(H_2O)_2]\cdot 6H_2O$; (**III**) $[Cu(C_9H_7O_3)_2(C_9H_6O_2)_2]$ and (**IV**) $[Zn(C_9H_7O_3)_2(C_9H_6O_2)_2(H_2O)_2]\cdot 3H_2O$. The ratio of metal: *p*-coumaric acid: coumarin in complexes are found to be 1:2:2. The complex **IV** is diamagnetic, and the other complexes are paramagnetic. According to BM data and result of electronic spectra, the geometry for all of the complexes has thought to be octahedral coordination around the metal ions.

Corresponding Authors
E-Mail: dalikose@hitit.edu.tr
Tel: +903642277000/1635
[a] Hitit University, Department of Chemistry, Ulukavak/Çorum, 19040
[b] Hitit University, Department of Molecular Biology and Genetic, Ulukavak/Çorum, 190402

Introduction

Coumarin (Coum), chemically 2H-chromene-2-one, belongs to the class of benzo[a]pyrones isolated from Tonka beans (Semen Tonca), removed from the tree called *Dipteryx odorata* (coumarone odorata), by Vogel in 1822. This species belongs to Fabaceae family and grows in South America.[1] The coumarin derivatives are present in various plants[2] such as Tonka bean, lavender, sweet clover grass and licorice and in food such as strawberries, cherries, apricots and cinnamon. Colored coumarin derivatives with fluorescencing properties are widely used in solar energy and laser systems.[3]

Several coumarin derivatives were isolated from various plants and microorganisms, and these generally were called after the name of the plant or place where the plant grown, which has resulted various trivial names for the same compound. For example, 7-hydroxycoumarin is also known as umbelliferone, skimmetin and hydrangea.[1] The coumarin has widespread application as an anticoagulant, spasmolytic and bacteriostatic agents and derivatives are also used as antibiotics, fungicides, anti-inflammatory, anticoagulant and anti-tumor agents.[2-4] The coumarin has sedative and anti-inflammatory effect and widely used in the perfumery and tobacco industry and as odorizer in some insecticides.[5] Coumarin and its metal complexes inhibit the proliferation of bacteria such as *Bacillus cereus*, *Pseudomonas aeruginosa* and *Escherichia coli*.[6] Coumarin plays an important role in the growth of plants because it inhibits enzymes such as amylase, invertase and stimulates oxidase and peroxidase enzymes.

The *p*-coumaric acid (p-CoumH) is derived from cinnamic acid and plays important role in color, odor and taste of several plant materials.[7] It is found in orange,[8] cherry, coffee, chocolate and wine.[9] It has been reported that *p*-coumaric acid provides protection against stress. Besides the ability to kill tumor cells, it has been reported that it may cause oxidative damage in DNA. In the case of taken in large amounts, it exerts toxic effect.[10] It is known that the *p*-coumaric acid is very effective against gastric cancer.

Experimental

In the synthesis of complexes, Coum and p-CoumH, obtained from Sigma-Aldrich, were used.

Monosodium salt of *p*-coumaric acid (p-CoumNa) was prepared by the reaction of 0.02 mol p-CouH and 0.02 mol of sodium bicarbonate solutions prepared in 50:50 (v/v) EtOH:H_2O. The solutions of starting materials are mixed and stirred until cessation of CO_2 evolution.

$$\text{p-CoumH} + NaHCO_3 = \text{p-CoumNa} + H_2O + CO_2 \quad (1)$$

The aqueous solution of metal salts (0.01 mol) and the solution of p-CoumNa (0.02 mol) were mixed and stirred at 55 °C for a day.

$$2\text{p-CoumNa} + M(NO_3)_2.xH_2O = M(\text{p-Coum})_2 + 2NaNO_3 + xH_2O \quad (2)$$

x=6 (Ni, Co); x=7 (Zn) and x=3(Cu);

The aq. EtOH=1:1 solution of p-coumaric acid transition metal salts (0.01 mol) was added to the 50:50 (v/v) EtOH: H_2O solution of coumarin (0.02 mol) and the mixture was stirred and refluxed approximately for a day.

$$M(p\text{-}Coum)_2+2Coum = [M(p\text{-}Coum)_2(Coum)_2(H_2O)_m].nH_2O \quad (3)$$

m=n=0 (Cu), m=2, n=3 (Zn), m=2, n=6 (Ni); m=2, n=4 (Co)

The solutions were allowed to stand at room temperature until crystallization. The resulting crystalline material was filtered off and dried at room temperature. The composition and structure of the complexes were investigated by the following methods.

Results and discussion

The transition metals salts of *p*-coumaric acid were synthesized in the reaction of monosodium salt of p-coumaric acid and the appropriate hydrated metal(II) nitrates in aqueous ethanol (1:1, v/v). These complexes were reacted with coumarine in aqueous ethanol (1:1, v/v), the yield and elemental analysis data of the new complexes synthesized (Co = (**1**), Ni = (**2**), Cu = (**3**), and Zn = (**4**)) are given in Table 1. The experimental and theoretical compositions of the synthesized complexes agreed well. The magnetic susceptibility of the products are in harmony with the literature data.[11-13]

Infrared Spectroscopy

The IR spectra of coumarine, *p*-coumaric acid and the synthesized mixed ligand complexes are given in Supplementary material (Figure S1) and the peak values and theirs assignation are given in Table 2.

The peak of stretching vibration belong to the C=O group of coumarine observed at 1753 cm^{-1} was shifted to 1704, 1706, 1697 and 1705 cm^{-1} in the spectra of Co^{II}, Ni^{II}, Cu^{II} and Zn^{II} complexes, respectively, as a result of coordination bond form between the carbonyl group and the metal cations.[14] Likewise, the peak observed for stretching of carboxylate C=O in *p*-coumaric acid was also shifted from 1688 cm^{-1} to 1621, 1620, 1628 and 1619 cm^{-1} in the spectra of Co^{II}, Ni^{II}, Cu^{II} and Zn^{II} complexes, respectively. The higher shifting values for *p*-coumaric acid comparing to coumarin ligand is the consequence of more ionic character of the bond between the metal and its ligand.[15,16] The most important indicator representing the denticity of carboxyilate group bonding is the difference between symmetrical and asymmetrical stretching vibrations of carboxylate groups. These differences were found to be 252, 248 and 255 cm^{-1} or the complexes of Co^{II}, Ni^{II} and Zn^{II} complexes, respectively, which show monodendate coordination mode of *p*-coumarate ligand, while the difference of 115 cm^{-1} for the Cu^{II} complexes unambiguously shows the bidendate coordination mode.[16,17]

Since the phenolic group of p-CoumH has not been deprotonated with $NaHCO_3$, two *p*-coumarate ligands are required to compensate the positive charge of the metal cation.

The other vibration bands of pyrone ring of coumarine appeared at 2910-2825 cm^{-1} (aromatic C-H) and 1522-1460 cm^{-1} (C-C vibrations). Stretching vibrations corresponding to the aromatic C-H bands were observed between 2860 and 2960 cm^{-1} in the mixed ligand complexes. The strong and broad band observed at 3600-3000 cm^{-1} belongs to the –OH group vibrations. The asymmetric and symmetric COO^- bands of carboxylate group are located between 1600-1610 cm^{-1} and 1380-1390 cm^{-1}, respectively. The absorption bands of the C-O groups can be observed between 890 and 900 cm^{-1}. The vibrations of metal-oxygen bonds belong to the pyrone and carboxylate oxygens could not be distinguished, the stretching vibrations were appeared at 610 and 526 cm^{-1} for Co^{II}; 611 and 526 cm^{-1} for Ni^{II}; 645 and 515 cm^{-1} for Cu^{II}, and 609 and 625 cm^{-1} for Zn^{II} complexes.[2,17,18]

Thermal Analysis

Thermal analysis curves of the complexes (TG, DTG, DTA) are given in Figure 1-4 and the results of thermal analysis are summarized in Table 3.

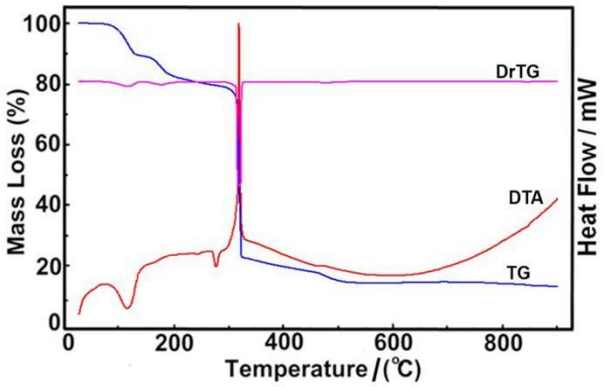

Figure 1. Thermal analysis curves of the complex $[Co(Coum)_2(p\text{-}Coum)_2(H_2O)_2].4H_2O$

The decomposition of the pink compound **I** consists of five steps as it can be seen from TGA curve. The decomposition temperatures are 84, 158, 236, 315 and 518 °C, respectively. The mass decrease of the first decomposition step confirm leaving of the 4 mol of crystallization water, the coordinated water (2 mol) leaves in the temperature interval of 123-182 °C

The organic ligands are lost between 185 and 345 °C, the final black product remained is CoO.

As it can be seen from Figure 2, the green Ni(II) complex decomposes in six steps at 75-131, 151, 210, 400 and 760 °C. The mass loss of the first of decomposition step corresponds the loosing of all six crystallization water. The coordinated water (2 mol) is lost between 142 and 165 °C. The ligand loss is occurred between 167 and 807 °C, the black residue was found to be NiO.

Table 1. The elemental analysis data of complexes

Complex	MW g mol^{-1}	Yield, %	Contents %,Found (calcd.)		Color	dec. °C	$\mu_{eff.}$ BM
			C	H			
$[Co(C_9H_7O_3)_2(C_9H_6O_2)_2(H_2O)_2]\cdot 4H_2O$ (**I**) $C_{36}H_{38}CoO_{16}$	785.61	89	55.72 (55.04)	5.23 (4.88)	Dark pink	84	3.52
$[Ni(C_9H_7O_3)_2(C_9H_6O_2)_2(H_2O)_2]\cdot 6H_2O$ (**II**) $C_{36}H_{42}NiO_{18}$	821.40	91	53.51 (52.64)	5.15 (4.88)	green	72	2.47
$[Cu(C_9H_7O_3)_2(C_9H_6O_2)_2]$ (**III**) $C_{36}H_{26}CuO_{10}$	682.13	95	62.92 (63.39)	3.77 (3.84)	blue	60	1.32
$[Zn(C_9H_7O_3)_2(C_9H_6O_2)_2(H_2O)_2]\cdot 3H_2O$ (**IV**) $C_{36}H_{36}ZnO_{15}$	774.04	86	57.59 (58.59)	5.11 (4.69)	white	71	Diam.

Table 2. IR spectra of the ligands and mixed ligand metal complexes

Groups	Coumarin	*p*-Coumaric acid	I (Co)	II (Ni)	III (Cu)	IV (Zn)
$\nu(OH)_{H2O}$	-	-	3600-3000	3600-3000	3600-2900*	3600-3000
$\nu(OH)_{carboxyl}$	-	3000-2900	-	-	-	-
$\nu(CH_2)$	2910,2825	2879,2685	2961,2857	2958, 2887	2956,2870	2931,2866
$\nu(C=O)_{carboxyl}$	-	1688	1621	1620	1628	1619
$\nu(C=O)_{pyrone}$	1753	-	1704	1706	1697	1705
$\nu(COO^-)_{asym.}$	-	-	1606	1605	1567	1604
$\nu(COO^-)_{sym.}$	-	-	1384	1386	1452	1382
$\Delta\nu_{asym-sym}$	-	-	252	248	115	255
$\delta(OH)_{H2O}$	-	-	1473	1467	1463	1486
$\nu(C-C)_{ring}$	1522,1460	1506,1432	-	-	-	-
$\nu(C-O)_{pyrone}$	917	-	893	896	886	891
$\delta(OH)_{carboxyl}$	-	973	-	-	-	-
$\nu(M-O)_{pyrone}$	-	-	610	611	645	609
$\nu(M-O)_{carboxyl}$	-	-	526	526	515	625

*Due to the –OH group of complex.

Table 3. The thermal analysis data for mixed ligand complexes

Complexes	Step	Temp. Interval, °C	DTA_{max}, °C	Leaving group	Weight loss %		Reside %		Decomp. product
					Exp.	Theo.	Exp.	Theo.	
I Co(II)									
	1	55-121	84	$4H_2O$	9.27	9.17			
	2	123-182	158	$2H_2O$	4.59	4.68			
	3	185-267	236	$2C_9H_8O;2C_6H_6O$	55.57	56.82			
	4	268-345	315	C_2H_2	6.12	6.63			
	5	352-650	518	CO_2	10.91	11.72	11.42	9.56	CoO
II Ni(II)									
	1	61-141	75; 133	$6H_2O$	13.32	13.15			
	2	142-165	151	$2H_2O$	4.48	4.39			
	3	167-248	210	$2C_9H_8O$	32.47	31.67			
	4	256-653	400	$2C_6H_6O$	21.33	22.65			
	5	657-807	760	$2C_3H_3O_2$	17.91	17.30	10.77	9,10	NiO
III Cu(II)									
	1	145-266	208; 250	$2C_9H_8O$	37.87	38.31			
	2	267-431	310; 408	$2C_6H_6O$	25.91	27.27			
	3	433-488	471	$2C_2H_2$	8.53	7.63			
	4	490-851	722	$2CO_2$	12.21	12.90	12.83	11.67	CuO
IV Zn(II)									
	1	60-101	92	$3H_2O$	6.09	6.97			
	2	156-194	185	$2H_2O$	4.16	4.65			
	3	205-360	288; 295	$2C_9H_8O$	34.26	33.59			
	4	363-418	393; 408	$2C_6H_6O$	22.13	24.03			
	5	420-772	707	$2C_2H_2$	7.12	6.72			
	6	773-826	812	CO_2	10.41	11.37	11.68	10.52	ZnO

 DOI: 10.17628/ecb.2016.5.132-137

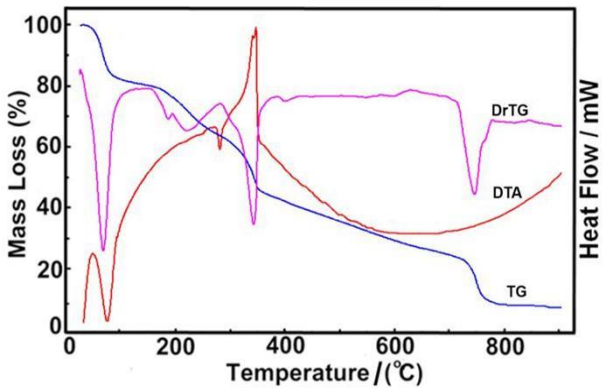

Figure 2. Thermal analysis curves of the complex $[Ni(Coum)_2(pCoum)_2(H_2O)_2].6H_2O$

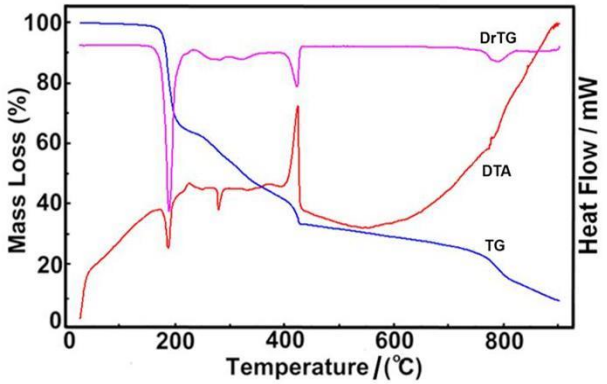

Figure 3. The thermal analysis curves of the complex $[Cu(Coum)_2(pCoum)_2]$

The compound **III** (Cu-complex) decomposes in four steps with at 208-250, 310-408, 471 and 722 °C. The first decomposition step is the main decomposition step with completely loss of ligands. Based on the mass decreasing, the supposed intermediate is copper(II) carbonate. Copper(II) carbonate decomposes in the temperature interval of 490-851 with formation of black CuO as final decomposition product.

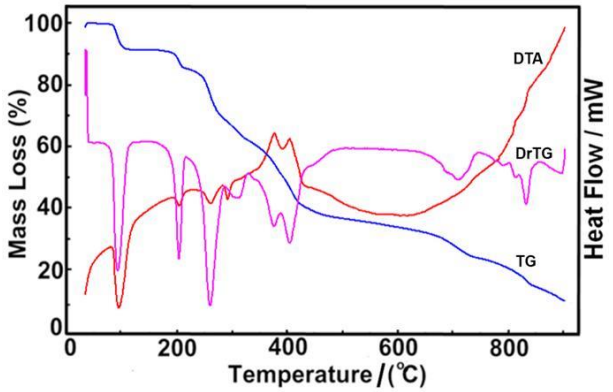

Figure 4. Thermal analysis curves of the complex $[Zn(C_9H_7O_3)_2(C_9H_6O_2)_2(H_2O)_2].3H_2O$

Complex **IV** decomposes in a six stage reaction at 92, 185, 288; 295-393; 408, 707 and 812 °C. The first decomposition step is the loss of 3 mol of crystalline water. The coordinated water (2 mol) is lost around 185 °C. The next steps belong to ligand loss when the final decomposition product is ZnO. The grey color of ZnO shows the presence of contamination from the organic ligand decomposition products.

Solid state UV–Vis spectroscopy

UV-visible spectra of the synthesized complexes were recorded between 900 and 200 nm (Figure 6). In case of complex I, the Co^{II} *d-d* transitions could be assignedto peak at 537.23 nm ($^4T_{1g}\rightarrow{}^4T_{2g}$) (F) and 469.45 nm ($^4T_{1g}\rightarrow{}^4T_{1g}$) (P).

Three spin-allowed *d-d* transitions of Ni(II) in the complex II were found at 821.52 nm ($^3A_{2g}\rightarrow{}^3T_{1g}$) (P), 684.87 nm ($^3A_{2g}\rightarrow\rightarrow{}^3T_{1g}$) (F) and 402.17 nm ($^3A_{2g}\rightarrow{}^3T_{2g}$) (F). Splitting of *d* orbitals confirms the octahedral geometry around the Ni(II) (Figure 4.20). The two of these transitions were found in the visible region, whereas the 402.17 nm ($^3A_{2g}\rightarrow\rightarrow{}^3T_{2g}$) (F) transition was shielded by the charge transfer bands.

The multiple absorption bands of the complex III were composed of overlapped peaks, and thus have a broad view in a wide range corresponding to the interval of 877.39-519.63 nm. According to these spectral data, it can be thought that the metal cation Cu(II) has a "pseudo-octahedral" structure with Jahn-Teller distortion. The maximum absorption band of a broad spectrum of the complex III corresponds to the wavelength value of approximately 709.71 nm ($^2E_g\rightarrow{}^2T_{2g}$) comes longitudinal waves.[18]

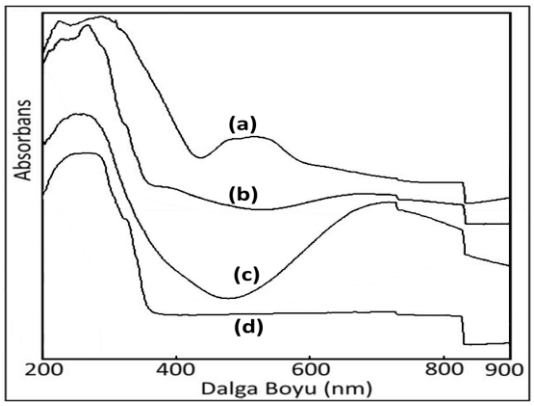

Figure 5. Solid State UV-vis spectra of the complexes. I-IV. **(a)** Co^{II}-complex, **(b)** Ni^{II}-complex, **(c)** Cu^{II}-complex, **(d)** Zn^{II}-complex

The zinc complex (IV) is diamagnetic and due to closed d-shells there are no d-d electronic transitions of the octahedral structure.[23]

 DOI: 10.17628/ecb.2016.5.132-137

Table 4. The *in vitro* antimicrobial activity of the complexes synthesized.

Complex	Strains (inhibition zones ±SD), mm				
	***S. aureus* ATCC 25923**	***E. faecalis* ATCC 29212**	***E. coli ATCC* 25922**	***P. aeroginosa* ATCC 27853**	***C. albicans* ATCC 0231**
I (Co)	10,0±2,0	9,0±1,0	-*	-	12,0±1,0
II (Ni)	-	10,0±0,1	-	-	11,0±1,0
III (Cu)	-	-	9,0±1,0	8,5±0,5	12,5±0,5
IV (Zn)	11,0±1,0	10,5±0,5	12,0±1,0	12,0±1,0	12,5±1,0

(*: no inhibition, the amount of complex used: 25 µl)

The high intensity absorption bands observed at lower wavelength belong to the metal → ligand charge transfer transition.[24] While the absorption bands of Co(II), Ni(II) and Cu(II) at the wavelength of 219.35 and 302.85 nm, 211.12 and 284.17 nm, and 257.61 nm belong to metal→ ligand transitions, the highly intensive peak observed in case of Zn complex (IV) at 281.15 nm could be assigned to ligand → metal charge transfer.[11-14,16-20]

Mass spectral analysis

The thermal decomposition pathway of the $[Ni(Coum)_2(pCoum)_2(H_2O)_2.6H_2O$ complex was recorded using direct insertion probe pyrolysis mass spectrometry method (Supplementary material, Figure S2). The mass spectra show the fragmentation pattern of the ligands, the molecular ion peak could not be detected.

Biological Application

The results obtained in studies of antimicrobial and total antioxidant activity (TAS) studies of the synthesized complexes are given in Table 4 and Table 5, and in the supplementary material (Figure S3).

Table 5. The results of total antioxidant activity for the complexes synthesized.

Metal complexes	Total antioxidant values (mmol Trolox Eq. L^{-1})
Co^{II} (**I**) complex	1.47
Ni^{II} (**II**) complex	1.33
Cu^{II} (**III**) complex	1.73
Zn^{II} (**IV**) complex	1.66

The coordination mode of ligands, the UV and magnetic measurements suggest octahedral geometry around the metal cations and water occupy the free coordination places in the complexes except the bidendate pCoum anion containing Cu(II) compound. The formula of the complexes can be written as follows as follows.

$$[M(Coum)_2(pCoum)_2(H_2O)_n].{}_mH_2O$$

M=Co, n=2, m=4 (**I**); M=Ni, n=2, m=6 (**II**); M=Cu, m=n=0 (**III**); M=Zn, n=2, m=3 (**IV**).

Among the studied mixed ligand complexes the lowest activity was observed for Ni^{II} (**II**) while the highest activity for Cu^{II} (**III**) complex. The strongest antimicrobial activity was found in case of Zn^{II} complex (**IV**).

Conclusion

Mixed ligand complexes of coumarine and *p*-coumaric acid with Co(II), Ni(II), Cu(II) and Zn(II) ions were synthesized and theirs structure were elucidated with using elemental analysis, infrared and ultraviolet-visible spectroscopy and magnetic measurements. The metal:ligand ratio was found to be 1: 2: 2 for all the complexes.

Acknowledgement

This research was supported by the Science Research Department of Hitit University (Project no: FEF.19004.13.002).

References

[1]Çamur, M., *Synthesis and characterization of structures some metal complexes of derivative of 4-hydroxyphenylacetic acid phatalocyanin using spectroscopic methods*, MSc Thesis, Marmara University, Science Institute, Istanbul, **2005**.

[2]Refat, M. S., El-Deen, I. M., Anwer, Z. M., El-Ghol, S., *J. Mol. Struct*., **2009**, *920*, 149.

[3]Alghool, S., *J. Coord. Chem.*, **2010**, *63(18)*, 3322.

[4]Mihaylov, Tz., Trendafilova, N., Kostova, I., Georgieva, I. and Bauer, G., *Chem. Phys.*, **2006**, *327*, 209.

[5]Kulkarni, A., Patil, S. A. and Badami, P. S., *Eur. J. Med. Chem.*, **2009**, *44*, 2904.

[6]Rehman, S. U., Chohan, Z. H., Gulnaz, F. and Supuran, C. T., *J. Enzyme Inhib. Med. Chem.*, **2005**, *20(4)*, 333.

[7]Kikugawa, K., Hakamada, T., Hasunuma, M. and Kurechi, T., *J. Agric. Food Chem.*, **1983**, 31(4), 780.

[8]Sousa, W. R., Rocha, C., Cardoso, C. L., Silva, D. H. S. and Zanoni, M. V. B., *J. Food Comp. Anal.*, **2004**, *17*, 619.

[9]Abdel-Wahab, M. H., El-Mahdy, M. A., Abd-Ellah, M. F., Helal, G. K., Khalifa, F. and Hamada, F. M. A., *Pharm. Res.*, **2003**, *48*, 461.

[10]Labieniec, M., T. Gabryelak, T. and Falcioni, G., *Mutation Res.*, **2003**, *539*, 19.

[11]Köse, D. A., Kaya, A. and Necefoğlu, H., *Russ. J. Coord. Chem.*, **2007**, *33(6)*, 422.

[12]İçbudak, H., Heren, Z., Köse, D. A. and Necefoðlu, H., *J. Therm. Anal. Cal.*, **2004**, *76(3)*, 837.

[13]Köse, D. A., Necefoğlu, H. and Içbudak, H., *J. Coord. Chem.*, **2008**, *61(21)*, 3508.

[14]Köse, D. A., Öztürk, B., Şahin, O. and Büyükgüngör, O., *J. Therm. Anal. Cal.*, **2014**, *115(2)*, 1515.

[15]Nakamoto, K., *Infrared and raman spectra of ýnorganic and coordination compounds, part b, applications in coordination, organometallic, and bioinorganic chemistry*. 6th Ed. John Wiley&Sons, Inc. New Jersey, **2009**.

[16]Koç, S., *Synthesis, structural characterization and biological application of mixed ligands complexes of coumaric acid/coumarine with some transition metal cations.* Msc Thesis, Hitit University, Science Institute, Çorum, **2014**.

[17]Köse, D. A., Şahin, O. and Büyükgüngör, O., *Eur. Chem. Bull.*, **2012**, *1(6)*, 196.

[18]Köse, D. A., Necefoğlu and H., Icbudak, H., *Hacettepe J. Biol. Chem.*, **2007**, *35(2)*, 123.

[19]Halli, M. B., Sumathi, R. B. and Kinni, M., *Spectrochim. Acta Part A*, **2012**, *99*, 46.

[20]Patil, S. A., Unki, S. N., Kulkarni, A. D., Naik, V. H. and Badami, P. S., *Spectrochim. Acta Part A*, **2011**, *79*, 1128.

Received: 28.04.2016.
Accepted: 07.06.2016.

DETERMINATION OF CAFFEINE CONTENT FROM DIFFERENT PHARMACEUTICAL AND NATURAL PRODUCTS

Andreia Corciova[a] and Bianca Ivanescu[b]*

Keywords: quantification, extraction, UV spectrophotometric methods, tablets, suppositories, green tea, black tea, coffee

The present study focuses on the quantification of caffeine from 11 pharmaceutical and natural products. Pharmaceutical products were purchased from pharmacy and include 4 types of tablets and 1 suppository type product. Natural products were purchased from specialty stores and comprise green tea, black tea and different kinds of coffee. Some of the quality parameters like friability and disintegration time for tablets, melting behavior, deformation temperature and time of deformation for suppositories were determined. The caffeine content was determined using UV spectrophotometric methods by measuring the absorbance at 272 nm, after separating the caffeine from the others active ingredients and excipients. The results showed that caffeine content in pharmaceutical products purchased from pharmacies is in the range recommended by European and Romanian Pharmacopoeia. In the case of natural products, the caffeine content decreases in the following order: bulk coffee beans freshly ground > ground coffee packed > black tea > green tea > decaffeinated coffee.

* Corresponding Authors
Fax: +40.232.211.820
E-Mail: biancaivanescu@yahoo.com
[a] "Grigore T. Popa" University of Medicine and Pharmacy Iasi, Faculty of Pharmacy, Department of Drugs Analysis, 16 Universitatii Street, RO-700115 Iasi, Romania
[b] "Grigore T. Popa" University of Medicine and Pharmacy Iasi, Faculty of Pharmacy, Department of Pharmaceutical Botany, 16 Universitatii Street, RO-700115 Iasi, Romania

Introduction

Caffeine ($C_8H_{10}N_4O_2$, 1,3,7-trimethylxanthine) (Figure 1) is a naturally occuring alkaloid that can be found in *Coffeae semen*, *Theae folium*, *Cacao semen*, *Colae semen*, *Mate folium* and *Paulliniae cupanae semen.* Due to its pharmacological effects, caffeine can also be found in different pharmaceutical products, associated for example with aspirin for treatment of headaches, with ergotamine for the antimigraine effect, with paracetamol and propyphenazone for pain relief or it can be used alone in the treatment of mild respiratory depression. Caffeine is a stimulant of central nervous system that reduces fatigue, increases attention and generates a faster and clearer flow of thoughts. When is consumed in moderate amounts, caffeine is good for health. It can reduce the risk of hepatocellular and endometrial cancer, and the risk of type 2 diabetes. Caffeine improves physical performance and sometimes is used as a doping substance by athletes. Furthermore, it has a bronchodilator effect attenuating asthma symptoms and a diuretic effect on the kidney.[1-6]

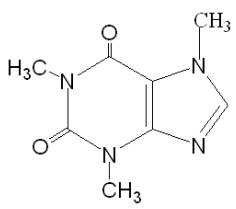

Figure 1. Caffeine structure

On the other hand, caffeine stimulates the stomach to produce large amounts of acid and aggravates peptic ulcers of stomach and duodenum. If it is consumed in large amounts can produce constriction of blood vessels, increase the blood pressure and provoke arrhythmia because of the cardiac stimulation. Also, caffeine elevates the levels of free fatty acids in the plasma and, when is overused, can exacerbate premenstrual symptoms. Caffeine crosses the placenta and if it is consumed during lactation may cause irritability and wakefulness in breastfed babies. When caffeine is consumed in quantities exceeding 250 mg per day can lead to nervousness, irritability, restlessness, insomnia, headaches and heart palpitations. This condition is named as caffeinism.[1-6]

For the determination of caffeine content from different matrices, various modern methods can be used: HPLC,[7-9] FTIR-ATR,[10] sequential perturbation caused by different amounts of caffeine on the oscillating chemical system in a continuous stirred-tank reactor (CSTR),[11] electrochemical detection of caffeine that uses a single-walled carbon nanotube on carbon-ceramic electrode (SWCNT/CCE).[12] Most of these methods are very complex and expensive, so we chose UV-VIS spectrophotometric method because is cheaper, rapid, simple and approachable in scientific teaching labs of school and universities.[3, 13-16]

The purpose of this paper was to determine the amount of caffeine in 5 pharmaceutical products and 6 natural products, using UV spectrophotometric methods.

Experimental

Materials

Caffeine standard was purchased from Sigma-Aldrich (Germania). All the chemicals used were analytical grade reagents. The pharmaceutical products used in the analysis were purchased from pharmacy and they correspond to 3 types of uncoated tablets containing, in addition to caffeine, aspirin and paracetamol (Sample 1); paracetamol and

propyphenazone (Sample 2); paracetamol, phenacetin and codeine (Sample 3); a type of effervescent tablet containing indomethacin and prochlorperazine (Sample 4) and a type of suppository containing indomethacin and prochlorperazine (Sample 5).

The natural products used for this analysis were purchased from specialty shops. The products used are green tea (Sample 6), black tea (Sample 7), bulk coffee beans which was freshly ground (Sample 8), ground coffee from producer 1 (Sample 9), ground coffee from producer 2 (Sample 10) and bulk decaffeinated coffee (Sample 11)

Equipment

A Jasco V 530 double beam UV-Vis spectrophotometer was used. All the measurements were made in 1.0 cm quartz cells at a scan speed of 1000 nm min^{-1} and scan range of 200 – 400 nm, fixed slit width of 2 nm.

Methods

First, caffeine was extracted using special conditions in order to separate it from other active ingredients or excipients that the product may contain. Determination of caffeine content in all samples was carried out by using a UV spectrophotometric method. The specific absorbance of caffeine was used for calculation of caffeine content in tablets while the external standard method was applied for suppositories and the calibration curve method was used for natural products.

Separation of caffeine from the samples

Sample 1 and 2 - To a quantity of powder corresponding to one tablet, 40 mL of water were added in a separatory funnel. The mixture was stirred for 5 minutes, then 5 mL of H_2SO_4 (0.05 mol) were added and caffeine was extracted three times with 20 mL of chloroform by shaking each time for 5 minutes. All chloroform phases were combined in another separatory funnel and were extracted again thrice using for each extraction 20 mL of NaOH (0.1 mol) and shaking for 5 minutes. The chloroform phase was filtered through anhydrous sodium sulfate and evaporated. The residue was quantitatively transferred into a 100 mL flask using HCl (0.1 mol). 2 mL of this solution was diluted with HCl (0.1 mol) to 100 mL, and the absorbance was measured at 272 nm using HCl (0.1 mol) as blank.[17]

Sample 3 - The same method was used to obtain the residue as for the previous samples. To the residue we added 0.1 g sodium benzoate and a small quantity of water. The solution containing the caffeine adduct was made up to a 100 mL flask using 0.1 M HCl. 2 mL from this solution was diluted with 0.1 M HCl to 100 mL, and the absorbance was measured at 272 nm using 0.1 M HCl as blank.

Sample 4 - To a quantity of powder corresponding to one tablet, 25 mL of neutralized alcohol were added. Then 2 drops of phenolphthalein were added and the titration was started using 0.1 M NaOH until a persistent pink colour was obtained. After the addition of an extra 5 mL of 10 % NaOH solution, the caffeine was extracted four times with 20 mL of chloroform. The chloroform phases were filtered through anhydrous sodium sulfate and evaporated. The residue was quantitatively transferred in a 100 mL flask using 0.1 M HCl. 2 mL from this solution were diluted with 0.1 M HCl to 100 mL, and the absorbance was measured at 272 nm using the solvent as blank.

For each pharmaceutical product presented as tablets, we crushed 20 tablets to a fine powder, after having first determined their average weight. Also, we determined some of the quality parameters like friability and disintegration time.[18,19] The caffeine content of tablets was calculated using a formula that includes: the absorbance of the sample, the specific absorbance of caffeine at 272 nm (470), the mass of powder used and the average weight of 20 tablets.

Sample 5 - The average weight of 20 suppositories was determined and after that the suppositories were pulverized and homogenized. An amount of powder equivalent to one suppository mass was extracted at high temperature using 10 mL of water and 2 g of paraffin. Next, the solution was cooled and filtered into a 50 mL volumetric flask. The procedure was repeated four more times using also the filter covered with residue; the flask was filled to the mark and the solution was homogenized. 1 mL from the final solution was diluted 50 mL with 0.1 M HCl and the absorbance was measured at 272 nm. A solution of 1 mg mL^{-1} caffeine was used as a standard. The caffeine content of suppositories was calculated using a formula that includes: the absorbance of the sample, concentration and absorbance of standard solution and the average weight of a suppository.

For the lipophilic suppositories we determined some of the quality parameters, such as melting behaviour, deformation temperature and also time of deformation .[18, 19]

Samples 6-11 - An exactly weighed amount of tea samples was infused for 30 minutes. For coffee samples decoctions were made by boiling the coffee for 5 minutes. The solutions were cooled and filtered. To 20 mL of each solution, 10 mL of 0.1 M HCl and 2 mL of basic lead acetate solution were added, and diluted with water to 250 mL. The resulting solution was filtered and 50 mL of it was mixed with 0.2 mL of 4.5 M H_2SO_4 and diluted to 100 mL with water. After mixing and filtration, the absorbance was measured at 272 nm.[3] The caffeine content of samples 6-11 was calculated using the calibration curve equation.

Results and Discussions

Table 1 shows the quality parameters for the analyzed tablets and Table 2 the quality parameters for suppositories.

Table 1. Quality parameters for the analyzed tablets.

Samples	Disintegration time (min)	Friability	Average weight (g)
1	9.0	0.2658 %	0.5161
2	2.0	0.2054 %	0.6496
3	5.0	0.4122 %	0.6497
4	1.5	0.512 %	1.8017

According to the European and Romanian Pharmacopoeia, the disintegration time in water, for uncoated compressed tablets must not exceed 15 minutes and for effervescent tablets 5 minutes. The friability should not be higher than 1 %. As shown by the results in table 1, the samples comply with the quality parameters.

Table 2. Quality parameters for suppositories

Samples	Melting behavior	Softening Temp.	Softening Time	Average Wt. (g)
5	20	38 ℃	3.45 min	1.5271

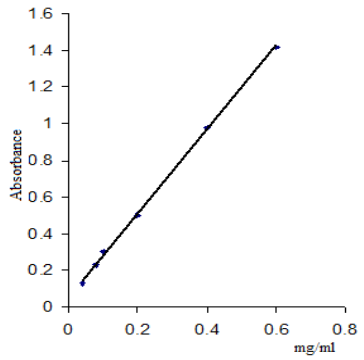

Figure 2. Calibration curve for caffeine.

The suppositories have to melt within 30 minutes, the softening temperature should be 37 ± 2 ^{0}C and the softening time should be at least 3 minutes. For Sample 5, the quality parameters are fulfilled.

The caffeine content of samples 6-11 was calculated using the calibration curve equation. In order to plot the calibration curve (Figure 2), a standard solution of caffeine 1 mg mL^{-1} was prepared and different solutions with concentrations between 0.04 – 0.6 mg mL^{-1} were made by dilution. Table 3 presents the statistical parameters for the determination of caffeine.

Table 3. Statistical data regarding caffeine determination.

Statistical Parameter	Value
Correlation Coefficient (r^2)	0.9993
Standard Error	0.014544
Intercept	0.0503
Slope	2.2943
Limit of detection	0.043834
Limit of quantification	0.132831

For each sample, the determinations were repeated three times, on three consecutive days. Table 4 presents the results for determination of caffeine content in pharmaceutical products expressed in mg per tablet and mg per suppository. Table 5 shows the caffeine content from natural products, expressed in g caffeine per 100 g tea or coffee.

Table 4. Caffeine concentration in pharmaceutical products

Conc. declared in per unit sample	Day 1		Day 2		Day 3	
	Conc. found	% Recovery	Conc. found	% Recovery	Conc. found	% Recovery
Sample 1	20.49	102.45	19.89	99.45	20.23	101.15
20 mg	20.56	102.8	20.18	100.9	19.97	99.85
	20.23	101.15	19.99	99.95	20.34	101.7
Average ± SD	20.42 ± 0.17	102.13 ± 0.86	20.02 ± 0.14	100.1 ± 0.73	20.18 ±0.19	100.9 ±0.95
Sample 2	51.02	102.04	49.96	99.92	50.12	100.24
50 mg	50.99	101.98	49.99	99.98	50.29	100.58
	50.97	101.94	50.01	100.02	50.07	100.14
Average ± SD	50.99 ± 0.025	101.98 ± 0.050	49.98 ± .025	99.97 ± 0.050	50.16 ± 0.11	100.32 ± .23
Sample 3	24.88	99.52	24.87	99.48	24.68	99.52
25 mg	24.79	99.16	24.92	99.68	24.23	99.16
	24.66	98.64	24.75	99	24.76	98.64
Average ± SD	24.77 ± 0.11	99.10 ± 0.44	24.84 ± 0.08	99.38 ± 0.35	24.55 ± 0.28	99.10 ± 0.44
Sample 4	76.01	101.34	76.4	101.86	76.35	101.8
75 mg	76.25	101.66	76.39	101.85	75.98	101.30
	76.35	101.8	76.28	101.70	76.71	102.28
Average ± SD	76.20 ± 0.17	101.60 ± 0.23	76.35 ± 0.06	101.80 ± 0.08	76.34 ± 0.36	101.79 ± .48
Sample 5	148.27	98.84	147.99	98.66	148.28	98.85
150 mg	148.1	98.73	147.29	98.19	148.66	99.10
	148	98.66	147.64	98.42	148.41	98.94
Average ± SD	148.12 ± 0.13	98.74 ± 0.09	147.64 ±0.35	98.42 ± 0.23	148.45 ± .19	98.96 ± 0.12

As seen in table 4, the recovery varies between 100.1 – 102.13 % (Sample 1), 99.97 – 101.98 % (Sample 2), 99.10 – 99.38 % (Sample 3), 101.60 – 101.80 % (Sample 4), 98.42 – 98.96 % (Sample 5). The limits established by Romanian Pharmacopoeia for tablets, where deviation depends on the caffeine content in each sample, are ± 7.5 %. For suppositories the permissible deviation is ± 5 %. So the variations are within the permissible range.

Table 5. Caffeine concentration in natural products (g $100g^{-1}$)

Sample No.	Concentration found, average ± SD		
	Day 1	Day 2	Day 3
6	1.016 ± 0.015	1.027 ± 0.004	1.005 ± 0.0223
7	1.08 ± 0.017	1.071 ± 0.004	1.076 ± 0.03
8	1.410 ± 0.009	1.408 ± 0.33	1.421 ± 0.19
9	1.373 ± 0.21	1.376 ± 0.08	1.369 ± 0.01
10	1.272 ± 0.039	1. 286 ± 0.59	1.277 ± 0.38
11	0.451 ± 0.040	0.442 ± 0.008	0.449 ± 0.04

The caffeine content in tea and coffee depends on the type of tea leaves, on the type of coffee beans, on the type of treatment and the method of preparation used. Generally, there is a higher content of caffeine in the tea leaves (3-5 %) than in coffee beans (1.35 - 2 %),[20, 21] but after the preparation of beverages there is a smaller content in tea than in coffee. That is probably because the coffee was boiled and the tea was infused. Another study compared the caffeine content of tea leaves and showed that the green tea has a caffeine content of 10-20 mg g^{-1} dried herb, while the black tea has a caffeine content of 22-28 mg g^{-1} dried herb.[22]

In our samples, the caffeine content of black tea is 1.071-1.08 % natural products, while the green tea has 1.005 – 1.016 % natural product. For the coffee samples, the content of caffeine varies in the range 1.272 - 1.421 % natural product, depending on the type of coffee used. Higher caffeine content was obtained when using bulk coffee beans freshly ground.

For decaffeinated coffee, the method for decaffeination is very important because in this process up to 97 % of the caffeine content is lost. The caffeine content in our sample is between 0.442 and 0.451 %.

Conclusions

All the analyzed pharmaceutical products conform to the requirements of European and Romanian Pharmacopoeia. There is a bigger quantity of caffeine content in the coffee samples than in the tea samples and in black tea than in green tea.

For the coffee samples, the caffeine content decreases in the following order: bulk coffee beans freshly ground > ground coffee from producer 1 > ground coffee from producer 2 > decaffeinated coffee.

References

[1]Cristea, A. N., *Tratat de farmacologie*, Editura Medicala, Bucuresti, **2012**.

[2]Ogah, C.O. and Obebe, O. T., *Int. J. Innovative Res. Eng. Sci.*, **2012**, *3(1)*, 404.

[3]Wanyika, H. N., Gatebe, E. G., Gitu, L. M., Ngumba, E. K. and Maritim, C. W., *Afr. J. Food. Sci.*, **2010**, *4(6)*, 353.

[4]Nawrot, P., Jordan, S., Eastwood, J., Rotstein, J., Hugenholtz A. and Feeley, M., *Food Addit. Contam.*, **2003**, *20(1)*, 30.

[5]Smith, A., *Food Chem. Toxicol*., **2002**, *40(9)*, 1243.

[6]Kraetsch, H. G., Hummel, T., Lotsch, J., Kussat, R. and Kobal, G., *Eur. J. Clin. Pharmacol.*, **1996**, *49(5)*, 377.

[7]Sharmin, R. C., Mahfuza, M. and Mahbubul, H. S., *Asian J. Pharm. Anal*., **2012**, *2(1)*, 01.

[8]Pandurang Patil, N., *Int. J. Pharm. Sci. Rev. Res*., **2012**, *16(2)*, 76.

[9]Chirita, R. I., Dascalu, C., Gavrila, L. and Elfakir, C., *Rev. Chim.*, **2010**, *61(12)*, 1173.

[10]Paradkar, M. M. and Irudayaraj, J., *J. Food Chem*., **2002**, *78(2)*, 261.

[11]Gao, J., Ren, J., Yang, W., Liu, X. H. and Yang, H., *J. Pharm. Biomed. Anal.*, **2003**, *32(3)*, 393.

[12]Habibi, B. and Abazari, M., *Chinese J. Catal*., **2012**, *33(11-12)*, 1783.

[13]Kuldeep, D., Ritu, K., Prachi, K., Sunil, K. and Pratik, P., *Int. J. Pharm. Pharm. Sci*., **2011**, *3(3)*, 170.

[14]Dinc, E., Kdil, G. K. and Onur, F., *J. Pharm. Biomed. Anal.*, **2001**, *26(5-6)*, 769.

[15]Kalra, K., Kumar, S. and Maithani, J., *Int. J. Pharm. Life Sci.*, **2011**, *2(11)*, 1214.

[16]Singh, D. K. and Sahu, A., *Anal. Bio. Chem*., **2006**, 349(2), 176.

[17]Muntean, D. L. and Imre, S., *Analiza medicamentului – ghid practic*, University Press, Tg. Mures, **2007**.

[18]*European Pharmacopoeia*, 8.0 edition, **2014**.

[19]*Romanian Pharmacopoeia*, 10.0 edition, *Editura Medicala, Bucuresti*, **1993**.

[20]http://www.polaris.nova.edu/~shanbhag/chemistry/oc1labs/caffeine.pdf

[21]http://www.caffeine-content.com/caffeine-in-coffee/caffeine-in-instant-coffee/

[22]http://www.energyfiend.com/caffeine-content/green-tea

Received: 03.04.2016
Accepted: 13.06.2016.

SYNTHESIS AND STRUCTURE OF NEW N-ALKOXY-N-(1-PYRIDINIUM)UREA CHLORIDES

V. G. Shtamburg,[a] V. V. Shtamburg,[b] A.V. Tsygankov,[c] A. A. Anishchenko,[d] R. I. Zubatyuk,[e] S. V. Shishkina,[e] A. V. Mazepa[f] and E. A. Klots[g]

Keywords: N-alkoxy-N-(1-pyridinium)urea salts, 1-N-alkoxyaminopyridinium salts, N-alkoxy-N-chloroureas, synthesis, structure.

New N-[1-(4-amino)pyridinium]-N-methoxyurea chloride, N-[1-(2-amino)pyridinium]-N-methoxyurea chloride and their analogs were synthesized by N-alkoxy-N-chloroureas reaction with the proper pyridines in acetonitrile or ether solution by improved procedure. XRD study of N-[1-(4-amino)pyridinium]-N-methoxyurea and N-[1-(2-amino)pyridinium]-N-methoxyurea revealed the elongation of N-N^+ bonds and some shortening of MeO-N bonds, qunonoid deformation of pyridine rings compare to it unsubstituted analog. The substantial pyramidality of central nitrogen atom in O-N-N^+ moiety and N-C carbamoyl bonds difference were established too. The structure summary of N-alkoxy-N-(1-pyridinium)ureas salts and other derivatives of 1-(N-alkoxyamino)pyridinium salts has been done.

* Corresponding Authors
Fax: (056) 374-98-41
E-Mail: koloxai@gmail.com; stamburg@gmail.com
[a] 49038 Ukraine, Dnepropetrovsk, Mostovaya st., 2/6. Ukrainian State University of Chemical Technology.
[b] 61050 Ukraine, Kharkov, Moskovsky pr., 31/56. Ukrainian State University of Chemical Technology.
[c] 25005 Ukraine, Kirovograd, Dobrovol'skogo st., 1. Kirovograd Flying Academy of National Aircraft University.
[d] 49010 Ukraine, Dnepropetrovsk, Armeyskaya st. 22 "b". Oles' Gonchar Dnepropetrovsk National University.
[e] 61001 Ukraine, Kharkov, Lenina ave., 60 . STC "Institute for Single Crystals", National Academy of Sciences of Ukraine.
[f] 65063 Ukraine, Odessa, Armeyskaya st. 21 . A.V. Bogatsky Physiko-Chemical Institute of NAS of Ukraine.
[g] 25006 Ukraine, Kirovograd, Shevchenko st., 1, V. Vinnichenko Kirovograd State Pedagogical University.

Introduction

1-(N-alkoxyamino)pyridinium salts were first synthesized by the interaction of N-chloro-N-methoxy-N-tert-alkylamines with pyridine.[1] The hygroscopic 1-(N-alkoxyamino)pyridinum chlorides are easily converted in the unhygroscopic perchlorates. These compounds may be regarded as a kind of N-alkoxyhydrazines. Usually such N-alkoxyhydrazines are labile due to destabilization by $n_{N'} \rightarrow \sigma^*_{N\text{-}O(R)}$ orbital interaction or anomeric effect.[2] But the 1-(N-alkoxyamino)pyridinum chlorides are relatively stable compounds due to impossibility of the orbital interaction caused by the absence of lone electron pair (LP) on nitrogen N'.

XRD study of the structure of perchlorate of 1-(N-methoxy-N-tert.alkyl)aminopyridinium[3] revealed a high degree of pyramidality of central nitrogen atom in the O−N−N^+ geminal system. The sum of bond angles centered on this nitrogen atom (∑β) is 322.8°. But the pyramidality of O−N−O central nitrogen atom in acyclic N,N-dialkoxyamine and in perhydro-1,3,2-dioxazepine is somewhat higher.[4] However, it was found by an XRD study[5] that in 1-(N-methoxy-N-tert.alkyl)amino-4-dimethylamino-pyridinium perchlorate, LP of central nitrogen is situated in pyridine plane (TaLPPy is 18°), its ∑β is 325.7°, the N−N^+ (1.445(2) Å) is shorter, and the N−OMe bond (1.425(2) Å) is longer. These structure changes reflect decreasing of action of $n_{O(Me)} \rightarrow \sigma^*_{N\text{-}N+}$ anomeric effect and stabilization of N−N^+ bond, respectively. These data are consistent with observed "quinonoid" deformation of pyridine ring in this compound. This phenomenon causes some difference in chemical properties of these classes of compounds. But reported structural data of N-alkoxy-N-(1-pyridinium)urea salts[5,6] are not sufficient for the complete understanding of this novel kind of anomeric urea salts. So, this work was undertaken to synthesize new N-alkoxy-N-(1-pyridinium)urea salts and to study of their structure.

Experimentals

^{1}H and ^{13}C NMR spectra were recorded on Varian VXP-300 spectrometer (300 and 75 MHz, respectively) and Varian JEMINI 2000 (400 and 100 MHz, respectively). Solvents were DMSO and CD_3OD with TMS as internal standard and expressed as δ ppm. IR spectra were recorded on UR-20 in KBr pellets. Mass spectra were recorded on VG 70-70EQ mass spectrometer in fast atom bombardment (FAB) mode. XRD structural study was performed on Xcalibur 3 automatic four-circle diffractometer (MoKα-radiation, graphite monochromator, Sapphire-3 CCD-detector, ω-scanning). Elemental analysis for C, H and N was performed on Carlo Erba analyzer.

4-Dimethylaminopyridine (DMAP), 4-aminopyridine and 2-aminopyridine were sublimated under vacuum (3 Torr). The solvents were purified and dried according to standard procedures.

N-[1-(4-Dimethylamino)pyridinium]-N-methoxyurea chloride (1)

A solution of DMAP (327 mg, 2.674 mmol) in Et_2O (30 mL) was added to a solution of N-chloro-N-methoxyurea (**2**)[7] (350 mg, 2.868 mmol) in Et_2O (5 mL) at -10 °C, the reaction mixture was maintained for 10 min at -10 °C, then 70 h at 5°C. The white precipitate was filtered off, washed with Et_2O (10 mL), then dried for 2 h under

vacuum (2 Torr), yielding **1** as white crystals (607 mg, 92 %). m.p. 168–169 °C (decomp.). which was identified by ^{1}H NMR spectroscopy and mass spectrometry.[5] ^{1}H NMR (300 MHz, CD_3OD) δ = 3.35 (6H, s, NMe_2), 3.88 (3H, s, NOMe) 7.07 (2H, d, ^3J = 7.8, H Py), 8.30 (2H, d, ^3J = 7.8, H Py). ^{1}H NMR (400 MHz, $(CD_3)_2SO$) δ = 3.28 (6H, s, NMe_2), 3.78 (3H, s, NOMe), 7.06 (2H, d, ^3J = 7.8, H Py), 7.96 (2H, br.s, C(O)NH_2), 8.44 (2H, d, ^3J = 7.8, H Py). ^{13}C NMR (100 MHz, $(CD_3)_2SO$) δ = 40.4 (NMe_2), 63.1 (NOMe), 107.5, 142.1, 156.6, 157.0 (C-2, C-3, C-4, C-5, C-6 Py), 255.8 (C=O). IR 1628 (C=N), 1725 (C=O), 3230 (N–H), 3300 (N–H) cm^{-1}. MS, *m/z* (%) = 211 [M+]$^+$ (100), 180 (27), 168 (8), 122 (14).

N-[1-(4-Amino)pyridinium]-N-methoxyurea chloride (3)

A solution of 4-aminopyridine (186 mg, 1.976 mmol) in MeCN (16 mL) was added to a solution of **2** (242 mg, 1.947 mmol) in MeCN (5 mL) at -30 °C. The reaction mixture was heated to 18 °C during 18 h, maintained for 2 h at 18°C, the precipitate was filtered off, washed with MeCN (4 mL), then CH_2Cl_2 (5 mL), dried under vacuum (2 mmHg), yielding **3** as yellowish-white hygroscopic crystals (408 mg, 95 %). m.p. 124–125 °C (decomp.)(i-PrOH). ^{1}H NMR (300 MHz, CD_3OD) δ = 3.88 (3H, s, NOMe), 6.93 (2H, d, ^3J = 7.5, H Py), 8.25 (d, 2H, ^3J = 7.5, H Py). ^{13}C NMR (75 MHz, CD_3OD) δ = 64.2 (NOMe), 110.7 (C-3, C-5 Py), 144.5 (C-2, C-6 Py), 162.5 (C-4 Py), 232.1 (C=O). IR 1660 (C=N), 1747 (C=O), 3310 ((N–H)$_2$), 3380 ((N–H) cm^{-1}. MS, *m/z* (%) = 183 M$^+$ (100). Anal. Calcd. for $C_7H_{11}ClN_4O_2$: C 38.45, H 5.07, N 25.62. Found: C 38.29, H 5.32, N 25.46.

N-[1-(2-Amino)pyridinium]-N-methoxyurea chloride (4).

A solution of 2-aminopyridine (194 mg, 2.055 mmol) in MeCN (6 mL) was added to a solution of **2** (253 mg, 2.035 mmol) in MeCN (6 mL) at -22 °C, the reaction mixture was heated to 9 °C for 16 h, maintained for 100 h at 12 °C, the white precipitate was filtered off, washed by benzene (4 mL), dried for 2 h under vacuum (5 Tor), yielding **4** as colourless hygroscopic crystals (288 mg, 65 %). m.p. 142–144 °C (decomp.)(i-PrOH). ^{1}H NMR (400 MHz, $(CD_3)_2SO$) δ, = 3.86 (3H, s, NOMe), 6.84 (1H, t, ^3J = 6.8 H Py), 7.40 (1H, d, ^3J = 8.4, H, Py), 7.83 (1H, t, ^3J = 8.0, H Py), 7.93 (1H, d, ^3J = 8.0 H Py), 7.96 (2H, s, C(O)NH_2), 9.04 (1H, s, NH_2 Py), 10.00 (1H, s, NH_2 Py). ^{1}H NMR (300MHz, CD_3OD) δ = 3.94 (3H, s, NOMe), 6.95 (1H, t, ^3J = 6.9 H Py), 7.17 (1H, d, ^3J = 9.0 H Py), 7.91 (1H, t, ^3J = 7.8 H Py), 8.01 (1H, d, ^3J = 7.2 H Py). ^{13}C NMR (75 MHz, CD_3OD) δ = 64.6 (NOMe), 115.3, 116.5, 137.6, 144.9 (C-3, C-4, C-5, C-6 Py), 158.0 (C-4 Py), 232.1 (C=O). MS, *m/z* (%): 183 M$^+$ (100). Anal. Calcd. for $C_7H_{11}ClN_4O_2 \cdot H_2O$: C 35.53, H 5.54, N 23.67. Found: C 35.44, H 5.65, N 23.46.

XRD structural study of compounds 3 and 4

Crystals, suitable for X-ray structural analysis, were grown from a solution in i-PrOH–MeOH mixture of **3** and from a solution of **4** in i-PrOH. The structure was solved by conjugate gradient technique with the SHELXD[8] software and refined by full matrix method of least squares in anisotropic approximation for non-hydrogen atoms SHELXL[8] software. The atomic coordinates, molecular geometry parameters, and crystallographic data of compounds **3** and **4** have been deposited in the Cambridge Crystallographic Data Center (deposits CCDC 1457353 (**3**) and 1457354 (**4**)).

N-[1-(4-Methyl)pyridinium]-N-methoxyurea chloride (5)

A solution of 4-methylpyridine (170 mg, 1.825 mmol) in Et_2O (4 mL) was added to a solution of **2** (167 mg, 1.341 mmol) in Et_2O (5 mL) at -34 °C, the reaction mixture was heated to 12 °C for 22 h, the white precipitate was filtered off, washed by Et_2O (6 mL), dried under vacuum (5 Torr) giving **5** as colorless hygroscopic crystals (163 mg, 56 %). m.p. 84–85 °C ($CHCl_3$) (decomp.). ^{1}H NMR (400 MHz, $(CD_3)_2SO$) δ = 2.72 (3H, s, Me,; 3.87 (3H, s, NOMe), 8.06 (2H, d, ^3J = 6.5, H Py,), 8.28 (2H, s, C(O)NH_2), 9.25 (2H, d, ^3J = 6.5, H Py,). ^{1}H NMR (300 MHz, CD_3OD) δ = 2.80 (3H, s, Me), 3.98 (3H, s, NOMe), 8.14 (2H, d, ^3J = 6.6, H Py,), 9.10 (2H, d, ^3J = 6.6, H Py). ^{13}C NMR (75 MHz, CD_3OD) δ = 22.9 (Me), 65.2 (NOMe), 130.5 (C-3, C-5 Py), 144.5 (C-2, C-6 Py), 158.9 (C-4 Py), 165.6 (C=O). MS *m/z* (%): 182 M$^+$ (100). Anal. Calcd. for $C_8H_{12}ClN_3O_2$: C 44.15, H 5.56, N 19.31. Found: C 43.98, H 5.82, N 18.65.

N-[1-(4-Dimethylamino)pyridinium]-N-ethoxyurea chloride (6a)

A solution of DMAP (92 mg, 0.753 mmol) in Et_2O (20 mL) was added to a solution of N-chloro-N-ethoxyurea (**7a**)[9] (115 mg, 0.828 mmol) in Et_2O (5 mL) at – 23 °C. The reaction mixture was heated to 13 °C for 20 h, maintained for 1 h at 17 °C, the precipitate was filtered off, washed with Et_2O (15 mL), dried under vacuum (3 Torr), giving **6a** as colorless crystals (187 mg, (5 %). M.p. 167–168°C (decomp.). ^{1}H NMR (300 MHz, $(CD_3)_2SO$) δ = 1.24 (3H, t, ^3J = 6.9, $NOCH_2\underline{Me}$), 3.29 (6H, s, NMe_2), 4.02 (2H, q, ^3J = 6.9, $NO\underline{CH_2}Me$,), 7.04 (2H, d, ^3J = 7.8, H Py), 7.28 (1H, br. s, C(O)NH_2), 7.99 (1H, br. s, C(O)NH_2), 8.48 (2H, d, ^3J = 7.8, H Py). ^{1}H NMR (300 MHz, CD_3OD) δ = 1.32 (3H, t, ^3J = 6.9, $NOCH_2\underline{Me}$), 3.34 (6H, s, NMe_2), 4.12 (2H, q, ^3J = 6.9, $NO\underline{CH_2}Me$,), 7.06 (2H, d, ^3J = 7.8, H Py), 8.30 (2H, d, ^3J = 7.8, H Py). ^{13}C NMR (75 MHz, CD_3OD) δ = 13.8 ($NOCH_2\underline{Me}$), 41.3 (NMe_2), 73.0 ($NOCH_2$), 109.0 (C-3, C-5 Py), 143.2 (C-2, C-6 Py), 159.0; 160.1 (C-4 Py), 232.1 (C=O). MS *m/z* (%) 225 M$^+$ (100), 180 (41), 164 (6). Anal. Calcd. for $C_{10}H_{17}ClN_4O_2$: C 46.07, H 6.57, N 21.49. Found: C 45.97, H 6.71, N 21.23.

N-[1-(4-Dimethylamino)pyridinium]-N-n-butyloxyurea chloride (6b)

A solution of DMAP (94 mg, 0.769 mmol) in Et_2O (18 mL) was added to a solution of N-n-butyloxy-N-chlorourea (**7b**)[6,10] (135 mg, 0.810 mmol) in Et_2O (5 mL) at 23 °C, The reaction mixture was maintained at 5°C for 22 h, the white precipitate was then filtered off, washed with Et_2O (6 mL), then with CH_2Cl_2 (15 mL), dried under vacuum (3 mmHg), giving **6b** as colorless crystals (141 mg, 63 %). m.p. 56–58 °C (decomp.). ^{1}H NMR (300 MHz, CD_3OD) δ = 0.91 (3H, t ^3J = 7.2, $NOCH_2CH_2CH_2\underline{Me}$), 1.37 (2H, sex, ^3J = 7.2, $NOCH_2CH_2\underline{CH_2}Me$), 1.69 (2H, quint, ^3J = 7.2,

$NOCH_2\underline{CH_2}CH_2Me$), 3.35 (6H, s, NMe_2); 4.09 (2H, t, ^3J = 7.2, $NO\underline{CH_2}CH_2CH_2Me$); 7.07 (2H, d, ^3J = 7.8, H Py), 8.31 (2H, д, ^3J = 7.8, H Py). ^{13}C NMR (75 MHz, CD_3OD, recorded in APT mode) δ = 14.1 ($NO(CH_2)_3\underline{Me}$), 41.0 (NMe_2), 108.9 (C-3, C-5 Py), 141.3 (C-2, C-6 Py), 19.9, 30.8 ($NOCH_2(\underline{CH_2})_2Me$), 77.2 ($NOCH_2$), 159.0 (C-4 Py), 232.2 (C=O). MS *m/z* (%): 253 M^+ (100), 210 (10), 179 (37), 124 (34). Anal. Calcd. for $C_{12}H_{21}ClN_4O_2$: C 49.91, H 7.33, N 19.40. Found: C 49.86, H 7.55, N 19.25.

Results and Discussion

We have synthesized novel amino-substituted pyridinium derivatives **3** and **4** by an interaction of **2** with 4-aminopyridine and 2-aminopyridine, respectively (Scheme 1).

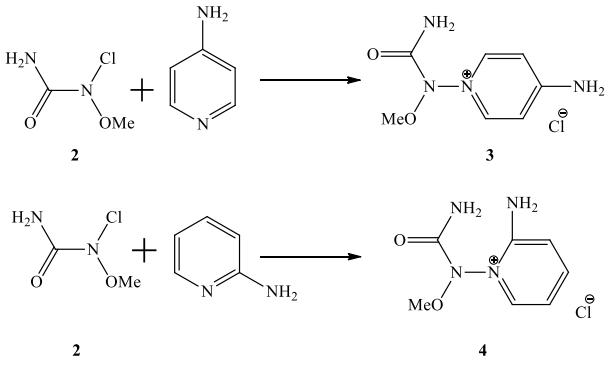

Scheme 1. Synthesis of compounds **3** and **4**.

This reaction has been carried out in MeCN solution, in which the products **3** and **4** are insoluble. In ether solution, **2** reacts with 4-methylpyridine to give **5**. N-alkoxy-N-chlorourea **7** and **8** yield **6a** and **6b** with DMAP (Scheme 2). Products **5**, **6a** and **6b** are insoluble in ether and appear as precipitates. As it analog **1** is sensitive to the presence of base,[11] N-alkoxy-N-chlorourea, **7** and **8** were used in excess in the syntheses of **6a** and 6**b**. This procedure avoids partial decomposition of the products. The known compound **1** can also be synthesized by this method.

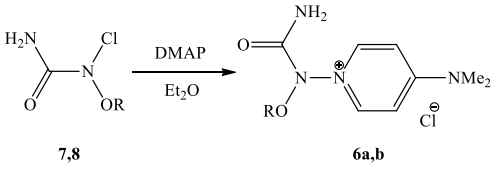

Scheme 2. Synthesis of compounds **6a** and **6b**. R = Et (**6a**, **7**), Bu (**6b**, **8**).

The structure of N-alkoxy-N-(1-pyridinium)urea chlorides **3, 4**, **5**, **6a** and **6b** was confirmed by ^{1}H and ^{13}C NMR spectroscopy, MS, and in the case of compounds **3** and **4** by XRD study also (Figure 1).

In the crystal, cations of compound **3** are linked in centrally symmetric dimmers by hydrogen bonds N1-H1a…O1^{i} [i: -x,1-y,-z] (H…O 2.09(2) Å, N-H…O 173.0(19)°). The dimmers are linked by intermolecular hydrogen bonds with Cl^- anions participating N1-H1b…Cl1^{ii} [-x,-y,-z] (H…Cl 2.74(3) Å, N-H…Cl 158(2)°), N4-H4a…Cl1^{iii} [iii: 1/2+x,1/2-y,-1/2+z] (H…Cl 2.39(3) Å, N-H…Cl 159(2)°), N4-H4b…Cl1^{iv} [iv: 1-x,-y,-z] (H…Cl 2.33(3) Å, N-H…Cl 170(2)°), C3-H3…Cl1^{v} [v: 1/2-x,1/2+y,-1/2-z] (H…Cl 2.68 Å, C-H…Cl 139°) and C7-H7…Cl1 (H…Cl 2.63 Å, C-H…Cl 155°). In compound **4** all intermolecular hydrogen bonds are formed with the participation of water and Cl^- anions: N1-H1b…O3^{i} [i: x,1/2-y,-1/2+z] (H…O 1.96(3) Å, N-H…O 173(2)°), O3-H3b…O1 (H…O 2.06(3) Å, O-H…O 162(3)°), N1-H1a…Cl1 (H…Cl 2.51(2) Å, N-H…Cl 157.2(18)°), O3-H3a…Cl1^{ii} [ii: -1+x,1/2-y,1/2+z] (H…Cl 2.28(4) Å, O-H…Cl 176(3)°), N4-H4a…Cl1^{iii} [iii: x,y,1+z] (H…Cl 2.34(2) Å, N-H…Cl 165(2)°), N4-H4b…Cl1^{iv} [iv: x,1/2-y,1/2+z] (H…Cl 2.53(3) Å, N-H…Cl 161(3)°) and C5-H5…O1^{v} [v: 1-x,-y,2-z] (H…O 2.55 Å, C-H…O 146°).

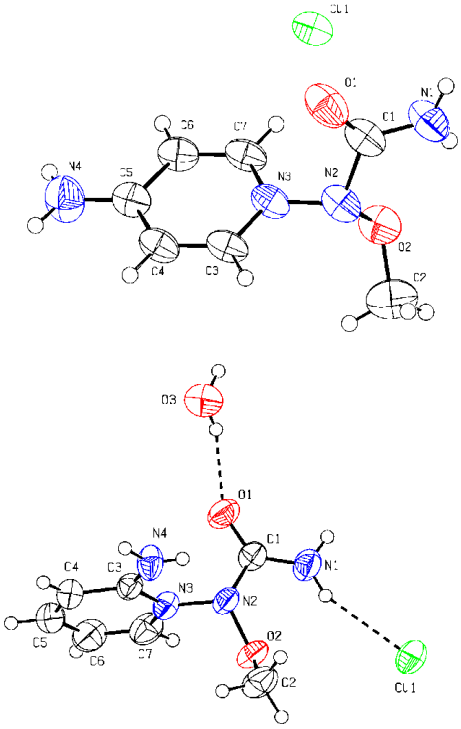

Figure 1. Molecular structure of **3** and **4** (monohydrate) with non-hydrogen atoms represented by thermal vibration ellipsoids of 50% probability.

In **3** and **4** central nitrogen atom of O–N–N^+ geminal system has trigonal-pyramidal configuration. In all cases its LP is situated in the plane of the pyridine circle. In compound **3** TaLPPy is equal to -1°, in compound **4** TaLPPy is 11°, the lengths of characteristic bonds are given in the Table 1.

In compounds **3** and **4** the carbamoyl moiety is oriented perpendicular to LP of N3 atom (the torsion angle O1-C1-N2-LP(N2) is -79° (**3**), -85° (**4**)), C-O bond of methoxy group is close to *sp*-orientation toward to LP of N3 atom (the torsion angle C2-O2-N2-LP(N2) is 22°(**3**), 18° (**4**)). In compounds **3** and **4** the weak intramolecular hydrogen bond N1-H1b…O2 takes place (H…O 2.20(2) Å (**3**), 2.28(2) Å (**15**), N-H…O 106(2)° (**3**), 102(2)° (**4**)). In compound **4,** N4 amino group is oriented to LP of N2 atom and forms a weak intramolecular hydrogen bond N4-H4b…N2 (H…N 2.39(3) Å, N-H…N 104(2)°).

 DOI: 10.17628/ecb.2016.5.142-146

Table 1. Structural parameters in N-alkoxy-N-(1-pyridinium)urea salts.

Compounds	∑β °	Bond lengths, Å			
		N−N$^+$	N−OMe	N−C(O)	R_2N'−C(O)
9[6]	333.9 (3)	1.425 (2)	1.400 (2)	1.452 (2)	1.323 (2)
1[5]	332.7	1.413 (2)	1.411 (2)	1.450 (2)	1.310 (2)
10[5]	324.22	1.425 (3)	1.429 (3)(Pr)	1.465 (3)	1.324 (3)
3	332.8 (4)	1.410 (2)	1.413 (2)	1.438 (2)	1.315 (3)
4	336.6 (4)	1.415 (2)	1.408 (2)	1.432 (2)	1.313 (2)

Note: **9** = 1-(N-methoxy-N-carbamoyl)aminopyridinium perchlorate, **10** = 1-(N-propoxy-N-dimethylcarbamoyl)amino-4-dimethylamino-pyridinium perchlorate

Table 2. Pyridinium ring deformation in N-alkoxy-N-(1-pyridinium)ureas salts **1**, **3, 4** and **10**.

Compounds	Bond lengths, Å			
	N1-C2, N1-C6	C2-C3, C5-C6	C3-C4, C4-C5	C4-NMe_2, C-NH_2
9[6]	1.341(2), 1.341(2)	1.385(3), 1.385(3)	1.349(5), 1.387(4)	-
1[5]	1.361(2), 1.345(2)	1.353(3), 1.341(3)	1.425(2), 1.426(2)	1.324(2)
10[5]	1.366(3), 1.346(3)	1.349(3), 1.334(3)	1.430(3), 1.413(3)	1.333(3)
3*	1.353(2), 1.356(2)	1.342(3), 1.343(3)	1.405(3), 1.421(3)	1.320(3)
4*	1.357(2), 1.374(3)	1.411(3), 1.336(3)	1.346(3), 1.402(3)	1.308(3)
Py[16]	1.337	1.380	1.379	C=N, 1.316

*Standard numeration of pyridine ring atoms has been used.

In the family of N-alkoxy-N-(1-pyridinium)ureas **1**, **3**, **4, 9** and **10** the largest degree of pyramidality of central nitrogen atom in O−N−N$^+$ germinal system is observed in compound **10.** Probably, it is caused by the presence of weak electronegative dimethylcarbamoyl substituent[2] at the nitrogen in contrast with the carbamoyl moiety present in other compounds. In compounds **1** and **3,** the nitrogen pyramidality degrees are similar (Table 1).

It must noted that N−C bond lengths in the family of N-alkoxy-N-(1-pyridinium)urea salts, **1**, **3, 4**, **9** and **10** are somewhat different (Table 1). The (AlkO)N−C(=O) bond is much longer, than N−C in urea[12] (1.350(1) Å) and in amides[13] (1.359 Å). But H_2N'−C(O) bond (or Me_2N'−C(O) bond in compound **10** is very short (Table 1). It results from different degrees of C=O conjugation with sp^3 hybridized nitrogen atom, N, and sp^2 hybridized nitrogen atom N'.[5]

The same difference of N−C carbamoyl bonds has been established for N-alkoxy-N-chlorourea,[7,14,15] N-acyloxy-N-alkoxyureas[6,9,13] and N,N-dialkoxyureas.[6,15]

In compound **3,** the presence of 4-amino group causes some N−OMe bond elongation and some N−N$^+$ bond shortening relatively to compound **9** (Table 1) and the known[5] quinonoid deformation of pyridine ring relatively to pyridine[16] and compound **9**[6] is established (Table 2). Thus it may be supposed that resonance form **3B** (Scheme 3) makes certain contribution to the structure of compound **14**. In form **3B** $n_N \rightarrow \sigma^*_{N\text{-}OMe}$ anomeric effect becomes possible. Its action is opposite to that of $n_{O(Me)} \rightarrow \sigma^*_{N\text{-}N+}$ anomeric effect, which dominate in resonance form **3A**.

In compound **4** a quinonoid deformation of pyridine ring is somewhat different, C4-C5 bond is shortened, C3-C4 bond is elongated, that is correspond with qinonoid form **4B** (Scheme 4).

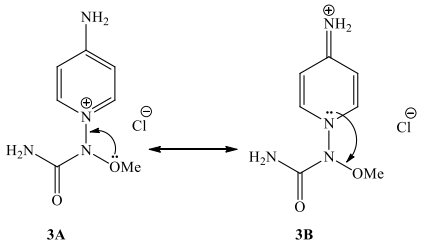

Scheme 3. Resonance in compound **3.**

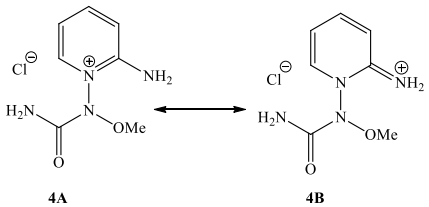

Scheme 4. Resonance in compound **4.**

Presence of 2-amino group in the pyridinium moiety causes some N−OMe elongation and any N−N$^+$ shortening relatively to compound **9** (Table 1). Probably, it is the concurrence of the sequence of $n_N \rightarrow \sigma^*_{N\text{-}OMe}$ and $n_{O(Me)} \rightarrow \sigma^*_{N\text{-}N+}$ anomeric effects.

In the case of both **3** and **4** C-NH_2, bond is shortened and its length is close to length of C=N$^+H_2$ bond.

It must be noted that quinonoid deformation of pyridine ring, similar to that observed in compound **3**, also takes place in 1-N-alkoxyamino-4-dimethylaminopyridinium salts[11] (Scheme 5).

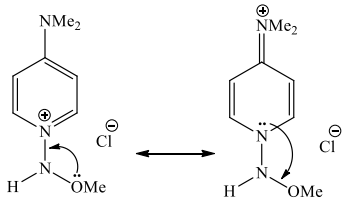

Scheme 5. Quininoid deformation in 1-N-alkoxyamino-4-dimethylaminopyridinium salts.

Conclusion

New N-[1-(4-amino)pyridinium]-N-methoxyurea chloride **3**, N-[1-(2-amino)pyridinium]-N-methoxyurea chloride **4** and their analogs were synthesized by an improved procedure. XRD study of N-[1-(4-amino)pyridinium]-N-methoxyurea and N-[1-(2-amino)pyridinium]-N-methoxyurea revealed the elongation of N-N^+ bonds and some shortening of MeO-N bonds, qunonoid deformation of pyridine rings compare to it unsubstituted analog. The substantial pyramidality of central nitrogen atom in O-N-N^+ moiety and N-C carbamoyl bonds difference was also established. The structural features of N-alkoxy-N-(1-pyridinium)urea salts and other derivatives of 1-(N-alkoxyamino)pyridinium salts has been summarized.

Acknowledgement

This work was supported by Department of Education and Science of Ukraine (grant no 0115U003159).

References

[1]Shtamburg, V. G., Rudchenko, V. F., Nasibov, Sh. S., Chervin I. I., Kostyanovsky, R. G., *Russ. Chem. Bull., Int. Edn.* **1981**, *30*, 1914-1920.

[2]Glover, S. A., *Tetrahedron* **1998**, *54*, 7229-7271.

[3]Shtamburg, V. G., Tsygankov, A. V., Klots, E. A., Fedyanin, I. V., Lyssenko, K. A., Kostyanovsky, R. G., *Mendeleev Commun*. **2006**, *16*, 84-85.

[4]Shtamburg, V. G., Klots, E. A., Gerasimenko, M. V., Shishkin, O. V., Zubatyuk, R. I., Kostyanovsky, R. G., *Mendeleev Commun*. **2011**, *21*, 349-350.

[5]Shtamburg, V. G., Tsygankov, A. V., Shishkin, O. V., Zubatyuk, R. I., Shtamburg, V. V., Gerasimenko, M. V., Mazepa, A. V., Kostyanovsky, R. G., *Mendeleev Commun*. **2012**, *22*, 92-94.

[6]Shtamburg, V. G., Shishkin O. V., Zubatyuk R. I., Kravchenko, S. V., Tsygankov, A. V., Shtamburg, V. V., Distanov, V. B., Kostyanovsky, R. G., *Mendeleev Commun*. **2007**, *17*, 178-180.

[7]Shtamburg, V. G., Shishkin, O. V., Zubatyuk, R. I., Kravchenko, S. V., Tsygankov, A. V.; Mazepa, A. V., Klots, E. A.; Kostyanovsky, R. G., *Mendeleev Commun*. **2006**, *16*, 323-325.

[8]Sheldrick, G. M., *Acta Cryst.* **2008**, *A64***,** 112-122.

[9]Shishkin, O. V., Zubatyuk, R. I., Shtamburg, V. G., Tsygankov, A. V., Klots, E. A., Mazepa, A. V., Kostyanovsky, R. G., *Mendeleev Commun*. **2006**, *16*, 222-223.

[10]Shtamburg, V .G., Klots, E .A., Pleshkova, A. P., Avramenko, V. I., Ivonin, S .P.; Tsygankov, A. V., Kostyanovsky, R. G., *Russ. Chem. Bull., Int. Edn.* **2003**, *52*, 2251-2260.

[11]Shtamburg, V. G., Shishkina, S. V., Shtamburg, V. V., Mazepa, A. V., Kadorkina, G. K., Kostyanovsky, R. G., *Mendeleev Commun*., **2016**, *26*, 169-171.

[12]Swaminathan, S., Craven, B. M., *Acta Cryst*. **1984**, *B40*, 300-306.

[13]Glover, S. A., White, J. M., Rosser, A. A., Digianantonio, K. M., *J. Org. Chem.* **2011**, *76*, 9757- 9763.

[14]Shishkin, O. V., Shtamburg, V. G., Zubatyuk, R. I., Olefir, D. A., Tsygankov, A. V., Prosyanik, A. V., Mazepa, A. V., Kostyanovsky, R. G., *Chirality*, **2009**, *21*, 642-647.

[15]Shtamburg, V. G., Kostyanovsky, R. G., Tsygankov, A. V.; Shtamburg, V.V., Shishkin, O. V., Zubatyuk, R. I., Mazepa, A. V., Kravchenko, S. V., *Russ. Chem. Bull., Int. Edn.* **2015**, 62-75.

[16]Burgi H.-B., Dunitz J. D., *Structure correlation*. Vol. 2. VCH. Weinheim. 1994, 741-784.

Received: 31.05.2016.
Accepted: 13.06.2016.

ETHYL SUCCINATE AND ETHYL-β-RIBOSIDE FROM *ACALYPHA WILKESIANA VAR. GOLDEN-YELLOW* (MUELL & ARG.)

Olawale H. Oladimeji[a]*, Emmanuel E. Attih[a] and Unwam-Abasi C. Udo[a]

Keywords: ethyl succinate, ethyl β-riboside, *A. wilkesiana var. golden-yellow* (Muell & Arg.).

Studies on chemical constituents of *A. wilkesiana var. golden-yellow* **(**Muell & Arg.) syn. *A. wilkesiana var. tropical tempest* used in traditional medicine, was carried out with solvent-partitioning of the aqueous extract of the plant with various organic solvents and subjecting the organic phases to silica gel column chromatography. Two compounds could be isolated from the butanol fraction which were assigned as 4-ethoxy-4-oxobutanoic acid (ethyl succinate) and 2-ethoxy-5(hydroxymethyl)-oxalane-3,4-diol (ethyl β-riboside) using the ^{1}H NMR, ^{13}C NMR, MS and IR spectral techniques. Both compounds were inactive against *B. subtilis*, *S. aureus* and *E. coli*. and showed minimal activity against *Ps. aeruginosa*, *S. typhi* and *V. cholerae*, and they had no anticandidal activity. The two isolates would serve as chemotaxonomic markers for this species and variety in particular and the genus, *Acalypha* in general.

Corresponding Author:
Tel: +2347038916740; +2348180035112; +2348173486285.
E-Mail: wale430@yahoo.co.uk; olawaleoladimeji@hotmail.com; hakeemoladmeji@uniuyo.edu.ng;)
[a] Department of Pharmaceutical & Medicinal Chemistry, Faculty of Pharmacy, University of Uyo, Uyo, Nigeria.

INTRODUCTION

Acalypha wilkesiana is named after the American scientist and explorer Admiral Chas Wilkes (1801-1877).[1] *A. wilkesiana var. golden-yellow* **(**Muell & Arg.) syn. *A. wilkesiana var. tropical tempest* is characterized by bright lime, yellow and green speckled leaves.[2-5] This variety possesses same morphological features as red acalypha variety which is predominately red and mottled with purple colourations. Different preparations of this plant are employed in folklore medicine in the treatment of malaria, wounds, tumours, inflammations, gastrointestinal disorders, bacterial and skin fungal infections.[6-11] Earlier, corilagin, geraniin, gallic acid, quercetin 3-O-rutinoside and kaempferol 3-O-rutinoside had been isolated from *A.wilkesina var. red acalypha* and *A. hispida* [12] while ethyl gallate, pyrogallol, D-arabino-hex-1-enitol and ethyl α-D-glucopyranoside had been obtained from *A. wilkesiana var. lace-acalypha.*[13-15]

In the present work studies have been carried out to isolate chemical constituents of the butanol fraction obtained from aqueous extract of the plant by column chromatography and also evaluate their antimicrobial potential. It is hoped that the obtained compounds may serve as chemotaxonomic markers for this species and variety in particular and genus, *Acalypha* in general.

Experimental

Collection of plant

The fresh leaves of *A. wilkesiana var.* golden-yellow **(**Muell & Arg.) were collected in the month of December, 2014 from a greenhouse facility located within the University of Uyo Town Campus, Uyo, Akwa Ibom State, Nigeria. A voucher specimen of the plant (No. H122) was deposited in the Herbarium Unit of the Faculty of Pharmacy. The plant was dried in an oven at 40 ^{0}C for 48 h and the resultant dried material powdered on an electric mill (Uniscope, England).

Extraction and isolation

The dried powder (0.85 kg) was exhaustively extracted with 50 % EtOH (4 x 5 L) at room temperature (27 ± 2 ^{0}C) for 72 h. The obtained crude extract was filtered, concentrated *in vacuo* on a rotary evaporator weighed and stored in a desiccator prior to further use. 107 g of the extract was partitioned using H_2O:1-butanol (6 x 500 mL). The resultant butanol fraction was evaporated to dryness to give a solid green residue. The butanol fraction (11.6 g) was chromatographed on a silica gel 254 (Merck, Germany) glass column (Techmel, USA; 10 g pre-swollen in 100 % toluene, 3 g concentration zone + 7 g separation zone, 16.5 x 3 cm) and eluted with a gradient of 10 % $(CH_3)_2CO$:toluene (60 mL), 20 % $(CH_3)_2CO$:toluene (60 mL), 30% $(CH_3)_2CO$:toluene (60 mL), 40 % $(CH_3)_2CO$:toluene (60 mL) and 50% $(CH_3)_2CO$: toluene (60 mL). Fractions of 8 mL each were collected, monitored on silica plates (Model No 64271, Merck, Germany) in $(CH_3)_2CO$:toluene:H_2O (10:20:1) using $FeCl_3/CH_3OH$ and vanillin-H_2SO_4 as spray reagents.

Subsequently, fractions with similar TLC characteristics (R_f values, reaction with $FeCl_3$ reagent or vanillin-H_2SO_4 spray) were combined and three semi-pure residues coded C-1, C-2 and C-3 were obtained. C-1 (1.4 g, deep green) was purified on a much shorter glass column (9.6 x 2 cm) isocratically with 100 % toluene (60 mL) resulting in 4-ethoxy-4-oxobutanoic acid (ethyl succinate) (olive green) coded **W-1** (R_f (0.76); 65 mg). Similarly, C-2 (1.1g, faintly greenish substance) was also cleaned on a short glass column using 20 % $(CH_3)_2CO$:toluene (80 mL) which yeilded 2-ethoxy-5-hydroxymethyloxalane-3,4-diol (ethyl β-riboside) (golden brown) **W-2** (R_f (0.58); 28 mg). C-3 (3.6 g, dirty white), a multi-component semi-pure residue was not processed any further in the course of the present study.

Structural elucidation

The mass spectra of the two compounds were obtained on Kratos MS 80 (Germany) while the infra-red analyses were done on Shimadzu FTIR 8400S (Japan). The ^{1}H and ^{13}C NMR spectra were obtained on Bruker AC 250 (Germany) operating 300 MHz for proton and 75 MHz for carbon-13 using CD_3OD as solvent and TMS as internal standard. Efforts were made to obtain the refractive indices of the compounds at the wavelength (λ) of Na-D line (589.3 nm) and at 20.5 ^{0}C [16-18] using the WAY-15 Abbe Refractometer (England).

Antimicrobial sensitivity screening

The microorganisms used in this study viz., *Bacillus subtilis* (NCTC 8853), *Staphylococcus aureus* (ATCC 25723), *Escherichia coli* (ATCC 25173), *Pseudomonas aeriginosa* (ATCC 2654), *Samonella typhi* (NCTC 5438), *Vibro cholerae* (ATCC 25032) and *Candida albicans* (NCYC 436) were clinically isolated from specimens of diarrheal stool, abscesses, necrotizing fascitis, osteomyelitis, urine, wounds and vaginal swabs obtained from the Medical Laboratory, University of Uyo Health Centre, Uyo. The clinical isolates were collected in sterile bottles, identified and typed by conventional biochemical tests.[19-20] These clinical microbes were then refrigerated at -5 ^{0}C at the Microbiology and Parasitology Unit, Faculty of Pharmacy prior to use. The agar plates used were prepared by adhering to the manufacturer's instructions. The media and plates were sterilized in an autoclave at 121 °C for 15 min. The hole-in-plate agar diffusion method was used observing standard procedure with Nutrient Agar-CM003, Mueller-Hinton-CM037 (Biotech Limited, Ipswich, England) and Sabouraud Dextrose Agar (Biomark, India) for the bacteria and fungus respectively. The inoculum of each micro-organism was introduced into separate petri-dish (Pyrex, England). Cylindrical plugs were removed from the agar plates by means of a sterile cork borer (Simax, India) to produce wells with diameter of approximately 6 millimetres. The wells were equidistant from each other and the edge of the plate.[21-22] Concentrations of 20 mg mL^{-1} of crude extract, 10 mg mL^{-1} of butanol fraction, 2 mg mL^{-1} of **W-1** and **W-2** were introduced into the wells. Also, different concentrations of 10 µg mL^{-1} chlorampenicol (Gemini Drugs, Nigeria), 1 mg mL^{-1} of nystatin (Gemini Drugs, Nigeria) and 50 % methanol were introduced into separate wells as positive and negative controls respectively.[13-15,23-24] The experiments were carried out in triplicates. The plates were labeled on the underside and left at room temperature for 2 h to allow for diffusion. The plates were then incubated at 37 ± 2 ^{0}C for 24 to 48 h. Zones of inhibition were measured in millimetres (mm) with the aid of a ruler.

Spectral data

W-1: $C_6H_{10}O_4$; amorphous olive green solid; R_f (0.76); 65 mg; $[n]^{20}_D$ (1.4333, 20.5 ^{0}C); MS [ES+-MS] m/z (relative intensity): 147 $[M+H]^+$ (0.34%) , 146 $[M]^+$ (0.76 %), 128 $[M-H_2O]^+$ (14.74 %), 119 $[M-C_2H_5)]^+$ (0.84 %), 101 $[M-COOH]^+$ (100.00 %) (base peak), 84 $[M-OC_2H_5-OH]^+$ (0.78 %), 73 $[M-OC_2H_5-CO]^+$ (27.12 %), 56 $[M-OC_2H_5-COOH]^+$ (12.77 %), 55$[M-OC_2H_5-COOH-1]^+$ (28.47 %), 29 $[M-COOC_2H_5-OC=O]^+$ (49.65 %) and 27 $[M-COOC_2H_5-COOH-1]^+$ (21.54 %); IR cm^{-1}: 719, 864 (fingerprint), 1721(-C=O) and 3219 (-OH); ^{1}H NMR δ (ppm): 0.98 (t) and 1.42 (q); ^{13}C NMR δ (ppm): 19.45 (methyl-C), 34.42 (methylene-C), 160.43 (carbonyl-C) and 162.59 (ester-C).

W-2: $C_7H_{14}O_5$; golden brown substance; R_f (0.58); 28 mg; MS [ES+-MS] m/z (relative intensity):178 $[M]^+$ (0.12 %), 147 $[M-CH_2OH]^+$ (0.67 %), 133 $[M-OC_2H_5]^+$ (0.54 %), 114 $[M-OC_2H_5-OH-2]^+$ (0.25 %), 101 $[M-OC_2H_5-CH_2OH-1]^+$ (0.46 %), 88 $[M-CH_2OH-2OH-25]^+$ (10.78 %), 71 $[M-CH_2OH-2OH-C_2H_5-13]^+$ (48.67 %), 60 $[M-CH_2OH-3OH-C_2H_5-7]^+$ (100.00 %) base peak), 47 $[M-CH_2OH-3OH-OC_2H_5-4]^+$ (40.87 %); IR cm^{-1}: 634, 756, 843 (fingerprint), 1052 (-C-O-C), 2937 and 3376 (-OH); ^{1}H NMR δ (ppm): 1.26 (t), 1.47 (q) and 5.15(s); ^{13}C NMR δ (ppm): 29.52 (methyl-C), 36.48 (methylene-C), 145.63 and 146.45 (hydroxylated-C).

The $[n]^{20}_D$ value of **W-1** was found to be 1.4333 which is particularly consistent with the literature value of 1.4328. The insufficient amount of **W-2** sample prevented establishing the refractive index unambiguously.

Table 1. Results of antimicrobial screening of crude extract, butanol fraction, **W-1** and **W-2** at different concentrations on test microbes in 50 % MeOH

Test microbe	CE, 20 mg mL^{-1}	BT, 10 mg mL^{-1}	W-1, 2 mg mL^{-1}	W-2, 2 mg mL^{-1}	50 % MeOH	CP, 10 µg mL^{-1}	NY,1 mg mL^{-1}
B. subtilis (NCTC 8853)	6	6	6	6	6	34	6
S. aureus (ATCC 25723)	6	6	6	6	6	35	6
E. coli (ATCC 25173)	6	6	6	6	6	36	6
Ps. aeriginosa (ATCC 26154)	7.6	7.8	7.8	7.8	6	31	6
S. typhi (NCTC 5438)	6	6	7.3	7.5	6	28	6
V. cholerae (ATCC 25032)	6	6	7.8	7.7	6	38	6
C. albicans (NCYC 46)	6	6	6	6	6	6	39

Key: The zone diameter recorded is zone of inhibition + size of cup (zone of inhibition +6) mm; **CE** = Crude ethanolic extract; **BT** = Butanol fraction; **CP** = Chloramphenicol; **NY** =Nystatin; **W-1 =** 4-ethoxy-4-oxobutanoic acid (ethyl succinate); W-**2 =** 2-ethoxy-5-(hydroxymethyl)oxalane-3,4-diol (ethyl β-riboside); **NCTC** - National Collection of Type Cultures, Central Public Health Laboratory, Colindale Avenue, London NW9, UK; **NCYC**- National Collection of Yeast Cultures, UK; **ATCC**- American Type Culture Collection**,** Washington, DC.

 DOI: 10.17628/ecb.2016.5.147-150

RESULTS AND DISCUSSION

The chemical structures of the compounds were established by a combination of spectroscopic techniques as mentioned above. The ^{1}H and ^{13}C NMR spectra of **W-1** and **W-2** were found to be consistent with literature values for the two known organic compounds namely 4-ethoxy-4-oxobutanoic acid (ethyl succinate) and 2-ethoxy-5-hydroxymethyloxalane-3, 4-diol (ethyl β-riboside),[28], respectively.

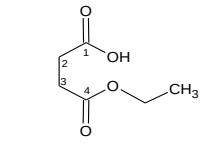

Ethyl succinate
(4-ethoxy-4-oxobutanoic acid)

W-1

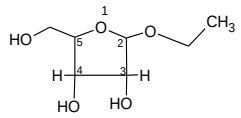

Ethyl β–riboside
(2-ethoxy-5(hydroxymethyl) oxalane-3,4-diol)

W-2

Due to the chemical nature of the matrices, a lot of fragmented ions appeared in the MS spectra of both compounds. In the MS of **W-1,** those that could readily be identified include; $[M]^{+}$ at m/z 146 (2.51 %) while fragments at 119 (0.84 %), 101 (100.00 %) (base peak), 73 (27.12 %) and 56 (12.77 %) corresponded to the losses of ethyl group, carboxylate group, ethoxy and carbonyl units and ethoxy and carboxylate groups, respectively. Other noticeable ions at 84 (0.78 %), 55 (28.47 %), 29 (49.65 %) and 27 (21.54 %) were *quasi*-peaks. Similarly, **W-2** showed numerous peaks in its MS matrix but there were easily identifiable ions including $[M]^{+}$ at m/z 178 (0.12 %), while fragments at 147 (0.67 %) and 133 (0.54 %) represented the excisions of hydroxy methyl and ethoxy units from the **W-2** molecule, respectively. Other ions found in its spectrum at 114 (0.25 %), 101(0.46 %), 88 (10.78 %), 71 (48.67 %), 60 (100.00 %) (base peak) and 47 (40.87 %) were *quasi*-peaks.

The IR spectrum of **W-1** showed diagnostic stretchings at 1721 and 3219 cm^{-1} which indicated -C=O and -OH groups respectively. The IR spectrum of **W-2** indicated diagnostic signals at 1052, 2937 and 3376 cm^{-1} which represented -C-O-C (ether linkage) and -OH functional groups respectively.

Antimicrobial tests

The microbes employed in the sensitivity tests reflected the entire antimicrobial spectrum encompassing gram positive, gram negative and fungal strains. The results displayed in the Table 1 show that both the crude extract and butanol fraction were largely inactive against the microorganisms. Furthermore, **W-1** and **W-2** recorded no activity against *B. subtilis*, *S. aureus* and *E. coli* while the two compounds demonstrated very minimal activity against *Ps. aeriginosa*, *S. typhi* and *V. cholerae*. The non-reactivity shown towards especially the gram negative bacteria such as *Ps. aeriginosa* was not surprising because these bacteria are well known for their unique resistance to antimicrobial agents. This resistance is believed to be due to the nature of the cell envelope of these organisms which unlike gram positive organisms possess a sophisticated three-layered envelope which does not allow permeation of external agents. Also, both compounds demonstrated no antifungal activity against *C. albicans.* This particular observation was not surprising because fungal strains such as *Candida spp*. limit the permeation of substances because of their integral structures which are pleomorphic and facultative in nature hence, resembling those of higher plants.[29]

CONCLUSION

This study reports isolation of 4-ethoxy-4-oxobutanoic acid (ethyl succinate) and 2-ethoxy-5-hydroxymethyloxalane-3,4-diol (ethyl β-riboside) from the *A. wilkesiana var. golden-yellow*. These compounds are expected to serve as chemotaxonomic markers for the species and variety in particular and the genus, *Acalypha* in general. However, both compounds were generally inactive against microbes employed.

ACKNOWLEDGEMENTS

The authors are grateful to I. Wahala of the National Research Institute for Chemical Technology (NARICT), Zaria, Nigeria for his assistance in obtaining the spectra of the compounds. Also, the role of E. Akpan, Principal Technologist, Pharmaceutical Microbiology Unit, Faculty of Pharmacy, University of Uyo, Uyo, Nigeria in the conduct of the antimicrobial screening is warmly appreciated. The authors are grateful to Dr. M. Bassey and O. Etefia, Department of Botany and Ecology and Department of Pharmacognosy and Natural Medicine, respectively, both of University of Uyo, Nigeria for their help in getting plant samples.

REFERENCES

[1]Bailey, L. H., *Manual of Cultivated Plants*, Macmillan Company, **1951,** 621-622.

[2]Hutchinson, J., Dalziel, J. M., *Flora of West Tropical Africa*. 1st edition., Volume 1, Part 2, *Crown Agents for Overseas Government and Administration*, **1958,** 408-410.

[3]Uphof, J. C., *Dictionary of Economic Plants*. H.R. Engelmann, **1959**, 5.

[4]Burkill, H. M., *The Useful Plants of West Tropical Africa*, 2nd edition, Royal Botanical Gardens, **1985**, 98-157.

[5]Watt, J. M., Breyer-Brandwijk, M. G., *The Medicinal and Poisonous Plants of Southern and Eastern Africa*, E. and S. Livingstone Limited, **1962**, 45.

[6]Oliver, B., *Medicinal Plants in Nigeria I*, Nigerian Coll. Arts, Sci. Technol., **1958,** 4-11.

[7]Oliver, B., *Medicinal Plants in Nigeria II*, Nigerian Coll. Arts, Sci. Technol., **1959,** 50-51.

[8]Akinde, B. E., Odeyemi, O. O., *Nigerian Med. J*., **1987,** *17*, 163-165.

[9]Alade, P. I., Irobi, O. N., *J. Ethnopharmacol*., **1993**, *39*, 171-174.

[10]Bussing, A., Stein, G. M., Herterich, A. I., Pfuller, U., J. *Ethnopharmacol*.**, 1999,** *66*, 301-309.

[11]Ikewuchi, J. C., Anyadiegwu, A., Ugono, E. Y., Okungbara, S. O., *Pak. J. Nutr.*, **2008**, *17(1)*, 130-132.

[12]Adesina, S. K., Idowu, O., Ogundaini, A. O., Oladimeji, H., Olugbade, T. A., Onawunmi, G. O., Pais, M., *Phytother. Res.*, **2000**, *14*, 371-374.

[13]Oladimeji, H. O., Igboasoiyi**,** A. C., (2014). *Afri. J. Pharmacol. & Therapeutics*, **2014**, 3(3), 79-84.

[14]Oladimeji, H. O., Udom, F. I., *Eur. Chem. Bull.*, **2014**, *3(11)*, 1060-1063.

[15]Oladimeji, H. O., Johnson, E. C., *J. Pharm. Bioresource*s, **2015**, *12(1)*, 48-53.

[16]Olaniyi, A. A., *Essential Medicinal Chemistr*y, 1st edition, Shaneson C. I. Limited, **1989**, 137-154.

[17]Olaniyi, A. A., Ogungbamila, F. O., *Experimental Pharmaceutical Chemistry*, Shaneson C. I. Limited, **1991**, 78-79.

[18]Olaniyi, A. A., *Principles of Quality Assurance and Pharmaceutical Analysis*, Mosuro Publishers, **2000**, 151-158, 216-217, 264-269 and 443-457.

[19]Gibson, L., Khoury, J., *Lett. Applied Microbiol*., 1986, *3*, 127-129.

[20]Murray, P., Baron, E., Pfaller, M., Tenover, F., Yolken, R., *Manual of Clinical Microbiology*, American Society of Microbiology Press, **1995**, 973.

[21]Washington, J., *The Agar Diffusion Method. In: Manual of Clinical Microbiology*. 4th edition, American Society of Microbiology Press, **1995**, 971-973.

[22]N. C. C. L. S., *Performance Standard for Antimicrobial Susceptibility Test*, 8th edition, Approved Standard, The Committee, **2003,** 130.

[23]Oladimeji, H. O., *Bioactivity-guided Fractionation of Acalypha wilkesiana (Muell & Arg.).* M. Sc.Thesis, Obafemi Awolowo University, Ile-Ife, **1997**, 98p.

[24]Oladimeji, H. O., *Chemical and Biological Studies on Cyathula prostrata (L.) Blume.* Ph. D. Thesis, University of Uyo, **2012**, 189p.

[25]Odebiyi, O. O., Sofowora, A., *Lloydia*, **1978**, *41***,** 234.

[26]Odebiyi, O. O., Sofowora, A., *Phytochemical Screening of Nigerian Medicinal Plants-Part II*. 2nd OAU/STRC Inter-African Symp. Trad. Pharm. African Med. Plants. OAU/STRC Publishers, **1979**, 216.

[27]Oladimeji, H. O., Usifoh, C. O., *J. Pharm. Bioresources*, **2015**, *12(2)*, 156-164.

[28]Lopez-Avila, V., *Org. Mass Spect*., **1987**, *22*, 557.

[29]Brown, M. R., *Pharm. J.*, **1975**, *215*, 239-242.

Received: 27.02.2016.
Accepted: 18.06.2016.

SYNTHESIS OF SOME NEW HETEROCYCLIC COMPOUND DERIVATIVES FROM 2-CHLORO-3-FORMYL-1,8,-NAPHTHYRIDINE

Ala Ismael Ayoub[a] and Mohanad Yakdhan Saleh[b]*

Keywords: Novel heterocycles, 1,8-naphthyridine , 1,3,4-oxadiazole, 1,3,4-thiadiazole, 1,2,4-trazole , Vilsmeier-Haack.

2-Chloro-3-formyl-1,8-naphthyridine (**1**) has been synthesized in a Vilsmeier-Haack type reaction route. Starting from (**1**) a number of novel 1,8-naphthyridines were also synthesized. The structures of synthesized compounds were confirmed by their spectral and physical data. Some of the newly synthesized compounds exhibited antibacterial activity.

* Corresponding Authors
Tel.: +9647701885033
E-Mail: mohanadalallaf@yahoo.com
[a] Department of chemistry , College of Sciences, University of Mosul, Iraq.
[b] Department of chemistry , College of Education for Pure Science, University of Mosul, Iraq

Introduction

1,8-Naphthyridine derivatives have attracted considerable attention as the 1,8-naphthyridine skeleton is present in many natural compounds show important biological activity.[1,2] For example, 2-amino-N-hydroxy-1,8-naphthyridine-3-carbox-amidine possesses herbicidal properties and used for selective control of weeds in barley, wheat, maize, sorghum and rice crops.[3] Some 3-phenyl-1,8-naphthyridine derivatives containing piperidyl , piperazinyl or morpholinyl group or an N-diethanolamine side chain show significant activity as inhibitors of human platelets aggregation induced by arachidonate and collagen.[4] Some 1,2,4-triazoles, 1,3,4-thiadiazoles and 1,3,4-oxadiazole derivatives have been attracting widespread attention due to their diverse pharmacological properties as anti-microbial, anti-inflammatory, analgesic and anti-tumor activities.[5-8.]

It is well known that the hydrazone group plays an important role in the bioactivity of hydrazone derivatives, e.g. a large number of hydrazones possessed interesting antibacterial and antifungal,[9,10] antiinflammatory,[11,12] and antimalarial[13] properties. With aim of obtaining new hydrazone derivatives with a wide spectrum of pharmaceutical applications, we have investigated the synthesis of new hydrazone derivatives[14,15,16] and theirs transformation into a series of heterocyclic compounds as 1,3,4-oxadiazole, 1,2,4-triazole and 1,3,4-thiadiazole derivatives of 1,8-naphthyridine.

EXPERIMENTAL

Melting points were recorded on electro-thermal CIA9300 melting point apparatus and are uncorrected, ^{1}H NMR spectra were recorded on a Bruker NMR spectrometer (300 MHz, Bruker Co., Germany), using TMS as internal reference and DMSO-d_6 as solvent. IR spectra were recorded on a Bruker Tensor 27 spectrometer by using KBr discs.

Synthesis of 2-chloro-3-formyl-1,8-naphthyridine (1)

To solution of (0.01mol) of N-(pyridine-2-yl)acetamide (0.15 mol) in dry DMF, $POCl_3$ (0.06 mol) was added dropwise with stirring at 0-5 °C.[17] The reaction mixture was refluxed for about 16 h with stirring. The reaction mixture was poured into crushed ice and the precipitated solid was filtered, washed with excess of cold water, dried and re-crystallized from ethanol (Scheme 1).

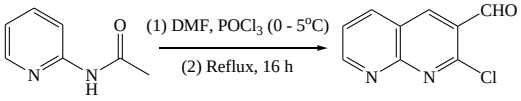

Scheme 1. Synthesis of 2-chloro-3-formyl-1,8-naphthyridine

Synthesis of 2-chloro-3-methoxycarbonyl-1,8-naphthyridine (2)

To a solution of (**1**) (0.01 mol) in methanol (10 mL) were added N-iodosuccinimide (NIS) (0.025 mol) and potassium carbonate (0.025 mol).[18] The resultant dark mixture was stirred in dark for 4 h. The reaction mixture was then diluted with 5-6 mL of water. Sodium thiosulphate (0.5 g) was added to destroy any remaining NIS or hypoiodite species. The solid product was filtered, dried and recrystallized from ethanol.

Synthesis of 2-chloro-1,8-naphthyridine-3-hydrazide (3)

To a solution of compound (**2**) (0.01 mol) in ethanol, hydrazine hydrate (6.5 mL) was added19 and the reaction mixture was stirred for 10 h at a temperature below 100 °C. The solvent was evaporated to half under reduced pressure. The precipitate which separated on cooling was collected by filtration and then recrystallized from ethanol.

Eur. Chem. Bull., **2016**, *5(4)*, 151-156 DOI: 10.17628/ecb.2016.5.151-156

Synthesis of 2-chloro-1,8-naphthyridine-3-thiosemicarbazide (4)

To an EtOH solution of hydrazide (**3**) (0.01 mol), NH4SCN (2.28 g, 0.03 mol) and cc. hydrochloric acid (4 mL) was added and stirred for 8 h at a temperature below 100 °C.[19] The solvent was evaporated under reduced pressure and the residue was poured on crushed ice. The solid formed was filtered and recrystallized from EtOH.

Synthesis of 2-chloro-3-[4-phenyl-1-acetyl thiosemicarbazide] -1,8-naphthyridine (5)

To ethanolic solution of hydrazide (**3**) (0.01 mole) phenyl isothiocyanate (0.02 mol), and concentrated hydrochloric acid (2 mL) was added and stirred for 10 h at a temperature below 100 ºC . The solvent was evaporated under reduced pressure and the residue poured on crushed ice with stirring. The solid formed was filtered and recrystallized from ethanol.

Synthesis of 2-chloro-3-[5-(1,2,4-triazolo-3-thione)]-1,8-naphthyridine (6)

To ethanolic solution of compound (**4**) (1.0 mmol), sodium hydroxide (0.056 g, 1.0 mmol) in 5 mL water was added and stirred for 6 h at 90 ºC.[19] The solution was filtered and neutralized with dilute hydrochloric acid. The crystalline material was filtered off and recrystallized from ethanol.

Synthesis of 2-chloro-3-[5-(2-amino-1,3,4-thiadiazolo)]-1,8-naphthyridine (7)

To a stirred solution of compound (**4**) (1.0 mol) in ethanol (50 mL), concentrated sulfuric acid (6 mL) was added and refluxed for 6 h at 90 ºC.[19] The solution was poured onto ice water, ammonia was added until it turns basic. A precipitate was obtained which was filtered and recrystallized from ethanol.

Synthesis of 2-chloro-3-[5-(2-phenyl amino-1,3,4-thiadiazole)]-1,8-naphthyridine (8)

To a stirred solution of compound (**5**) (1.0 mol) in ethanol (50 mL), concentrated sulfuric acid (6 mL) was added and refluxed for 6 h at 90 ºC. The solution was poured onto ice water, ammonia was added until it turns basic. A precipitate was obtained which was filtered and recrystallized from ethanol.

Synthesis of 2-chloro-3-[5-(4-phenyl-1,2,4-triazole-3-thione)]-1,8-naphthyridine (9)

To ethanolic solution of compound (**5**) (0.01 mole), sodium hydroxide (0.056 g, 0.01 mole) in 5 mL water was added and stirred for 8 h at 90 ºC. The resulting solution was acidified with 10% hydrochloric acid with cooling. The precipitate then filtered and recrystallized from ethanol.

Synthesis of 2-chloro-3-[5-(2-phenyl amine-1,3,4-oxadiazole)]-1,8-naphthyridine (10)

To solution of compound (**5**) (0.01 mol) in methanol (30 mL) , mercuric oxide (2.4 g , 0.01 mol) was added then the mixture was refluxed for 8 h and filtered while the solution is hot. The solvent was evaporated to give solid product which was dried and recrystallized from ethanol.

Synthesis of 2-chloro-N-formyl-1,8-naphthyridine-3-carbohydrazide (11)

A mixture of acid hydrazide (**3**) (0.01 mol) and formic acid (0.246 g, 0.01 mol) in ethanol (20 mL) was refluxed for 6 h.[13] On cooling a solid appeared, which was filtered, dried and recrystallized from ethanol.

Synthesis of N-benzylidene-2-chloro-1,8-naphthyridine-3-carbohydrazide (12)

A mixture of acid hydrazide (**3)** (0.01 mol) and benzaldehyde (0.01 mol) in ethanol (20 mL) was refluxed for 6 h. The solvent was evaporated and the precipitate filtered and recrystallized from ethanol.

Synthesis of 2-chloro-3-(1,3,4-oxadiazol-2-yl) -1,8-naphthyridine (13-14)

To separate homogenous solutions of carbohydrazide (**11**) and (**12**) (0.01 mol) in glacial acetic acid, PbO_2 (2.34 g, 0.01 mole) was added the mixture then stirred at 25 ºC for 4 h. The reaction mixture was diluted with ice-water and left to stand for 24 h. The precipitate was filtered, washed well with cold water and recrystallized from ethanol.

Synthesis of 2-chloro-3-[5-(1,3,4-oxadiazolo-2-thione)]-1,8-naphthyridine (15)

To ethanolic solution of hydrazide (**3**) (1.0 mmol), potassium hydroxide (0.056 g, 1.0 mmol) and carbon disulfide (2 mmol) was added. The mixture was heated under reflux until the evolution of hydrogen sulfide ceased.[19] The solvent was then removed, water was added and the solution was filtered off. The filtrate was acidified with diluted hydrochloride acid. The precipitate formed was collected, washed with water and recrystallized from ethanol.

Some physical properties and spectral data of compounds (**1**) – (**15**) are presented in Table 1 and 2.

RESULTS AND DISCUSSION

Although many reaction routes have been developed for functionalized 1,8-naphthyredines,[20,21,22] the Vilsmeier approach is found to be the most efficient for achieving useful transformation and heteroannulations.

 DOI: 10.17628/ecb.2016.5.151-156

Thus in this communication we have reported the synthesis of 2-chloro-3-formyl-1,8-naphthyridine from the reaction of N-(pyridin-2-yl)acetamide with Vilsmeier reagent and transformation of 2-chloro- and 3-formyl groups into different functionalities.

The Vilsmeier cyclization of N-(pyridin-2-yl)acetamide was carried out by adding $POCl_3$ to the substrate in DMF at (0-5 ºC) following by heating the mixture until 90ºC to afford 2-chloro-3-formyl-1,8-naphthyridine. The mechanism of reaction is given in Scheme 2.

Structures of synthesized compounds were elucidated by mean of physical data (Table 1).

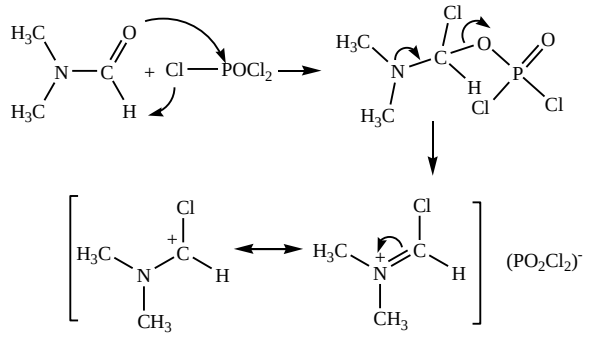

Scheme 2. The mechanism of Vilsmeier-Haack reaction.

The IR spectrum of compound (**1**) showed a sharp absorption at 1705 cm^{-1} belongs to the aldehyde group and an absorption band at 2820 cm^{-1} belongs to the aldehyde proton and an absorption band at 765 cm^{-1} for C-Cl group. Its ^1H NMR spectrum shows a singlet at δ = 9.83 and 7.26 for aldehyde and C-H protons, respectively, two doublets at 8.49 and 7.48 for C-7 and C-5 protons and a triplet at δ 7.31 for C-6 proton.

The formyl group was first oxidized to an ester group. Among the various available methods,23 the conversion of formyl group was made with using of N-iodosuccinimide(NIS)-K_2CO_3 mixture in methanol at room temperature to afford the corresponding 2-chloro-3-methoxycarbonyl-1,8-naphthyridine (**2**) in good yield (Scheme 3). The IR spectra of the compound (**2**) showed a strong absorption band at 1732 cm^{-1} belongs to the carbonyl group of the ester formed. The ^1H NMR spectrum of the compound showed a singlet at δ 4.3 and 7.92 for methoxy and C-4 hydrogens, respectively, two doublets at δ 7.42 and 8.38 for C-5 and C-7 protons and a triplet at δ 7.27 for C-6 proton.

The methyl ester (**2**) formed was treated with hydrazine hydrate in ethanol to give the corresponding acid hydrazide (**3**). The hydrazide group shows an absorption band at 3410 cm^{-1} for N-H and at an other at 1680 cm^{-1} for C=O group .

Table 1. Physical and IR Spectral data of compounds (**1**) – (**15**).

Comp No.	M.p. °C	Yield %	Formula	C=O	C=N	NH	C=S	C-H (aromatic)	C-O-C	C-Cl
1	165-167	60	$C_9H_5N_2OCl$	1705	1580	----	----	3085	----	765
2	96-98	65	$C_{10}H_7N_2O_2Cl$	1732	1618	----	-----	3040	----	770
3	172-175	60	$C_9H_7N_4OCl$	1680	1620	3410	----	3035	----	775
4	235-238	65	$C_{10}H_8N_5OSCl$	1690	1585	3252	1210	3083	----	768
5	252-254	60	$C_{11}H_{12}N_5OSCl$	1695	1575	3380	1220	3066	----	775
6	256-259	55	$C_{10}H_5N_5SCl$	----	1587	-----	1235	3045	----	780
7	246-249	55	$C_{10}H_5N_6SCl$	----	1595	3423	----	3035	----	768
8	269-271	55	$C_{16}H_{10}N_5SCl$	----	1605	3225	----	3056	----	780
9	252-254	60	$C_{16}H_{10}N_5SCl$	---	1529	3286	1210	3085	----	775
10	273-275	55	$C_{16}H_{10}N_5ClO$	---	1605	3380	----	3080	1210	778
11	221-223	60	$C_{10}H_7N_4ClO_2$	1715, 1685	1585	3380, 3315	----	3035	----	785
12	230-232	55	$C_{16}H_{11}N_4ClO$	1675	1605	3325	----	3035	----	775
13	274-276	50	$C_{10}H_4N_4OCl$	----	1595	---	----	3055	1085	720
14	268-271	50	$C_{16}H_9N_4OCl$	---	1605	----	----	3035	1125	780
15	212-215	45	$C_{10}H_5N_4OSCl$	----	1575	3325	1225	3085	----	775

 DOI: 10.17628/ecb.2016.5.151-156

Table 2. ^{1}H NMR data of compounds (**1**) – (**15**).

Comp. No.	^{1}H NMR δ ppm, Solvent: DMSO-d_6
1	7.31(1H, t, C-6-H), 7.48(1H, d, C-5-H), 7.86(1H, s, C-4-H), 8.49(1H,d, C-7-H), 9.83(1H, s, CHO)
2	4.3(3H , s , OCH_3) , 7.27-7.31(1H, t, C-6-H), 7.41-7.47(1H, d, C-5-H), 7.42(1H,s, C-4-H), 8.38-8.40(1H, d , C-7-H)
3	4.70(2H, s , NH_2) 7.33-735(1H, t, C-6-H), 7.45-7.47(1H, d, C-5-H), 8.01(1H, s , C-4-H), 8.42-8.44(1H, d , C-7-H), 9.95(1H, s, NH)
4	4.56-4.59(2H , s , NH_2), 7.56-7.59(1H, t, C-6-H), 7.83-7.86(1H, d-C-5-H), 8.01(1H, s ,C-4-H), 8.56-8.59(1H, d, C-7-H), 8.96(1H, S, NH) , 10.01(1H ,S, NH)
5	7.25-7.32(5H, m ,Ar-H), 7.58-7.60(1H, t, C-6-H), 7.84-7.85(1H, d, C-5-H), 7.94(1H, s , C-4-H), 8.59-8.61(1H, d , C-7-H), 8.84(1H, s , NH), 9.16(1H, s,NH), 10.56(1H , s , NH)
6	7.357.37(1H, t, C-6-H), 7.52-7.54(1H, d, C-5-H), 7.88(1H, s , C-4), 8.55-8.57(1H, d , C-7-H), 10.0 (1H, s , NH)
7	4.56(2H, s , NH_2), 7.33-7.35(1H, t, C-6-H), 7.48-7.51 (1H, d, C-5-H), 7.85(1H, s , C-4-H), 8.32-8.35(1H, d , C-7-H)
8	4.68(1H , s , NH), 7.11-7.32(5H , m , Ar-H), 7.36-7.37(1H, t, C-6-H), 7.51-7.53 (1H, d, C-5-H), 7.88(1H, s , C-4-H), 8.36-8.38(1H, d , C-7-H)
9	7.18-7.35(5H , m , Ar-H), 7.41-7.43(1H, t, C-6-H), 7.72-7.74(1H, d, C-5-H), 7.95(1H, s , C-4-H), 8.36-8.38(1H, d, C-7-H), 10.65 (1H, s , NH)
10	4.85(1H, s , NH), 7.21-7.31(5H , m , Ar-H) , 7.30-7.33(1H, t, C-6-H), 7.44-7.46 (1H, d, C-5-H), 7.81(1H, s , C-4-H), 8.29-8.31(1H, d , C-7-H)
11	4.85(1H , s , NH), 7.12-7.21(5H , m , Ar-H), 7.30-7.33(1H, t, C-6-H), 7.44-7.46 (1H, d, C-5-H), 7.81(1H, s , C-4-H), 8.29-8.31(1H, d , C-7-H)
12	6.23-6.25(1H , m , =CH), 7.12-7.24(3H , m , Ar-H), 7.35-7.38(1H, t, C-6-H), 7.46-7.48(1H, d , C-5-H), 7.85(1H, s , C-4-H), 8.33-8.35(1H, d , C-7-H), 9.05(1H , s , NH)
13	7.31-7.33(1H, t, C-6-H), 7.39-7.41 (1H, d-C-5-H), 7.81(1H,s , C-4-H), 7.95(1H , s , heterocyclic proton), 8.28-8.30(1H, d , C-7-H)
14	711-723(5H, m , Ar-H), 7.31-7.33(1H, t, C-6-H), 7.49-7.51(1H, d ,C-5-H), 7.86(1H, s , C-4-H), 8.42-8.44(1H, d , C-7-H)
15	7.29-7.31(1H, t, C-6-H), 7.46-7.48 (1H, d , C-5-H), 7.83(1H, s , C-4-H), 8.40-8.42(1H, d , C-7-H), 9.68 (1H, S, N-H)

The ^{1}HNMR spectrum of compound (**3**) showed absorption a singlet at δ 9.70 for NH_2 proton and at δ 7.33 ,7.45 , 8.01 and 8.42 for C-6 , C-5 , C-4 , C-7 proton respectively and at at δ 9.95 for NH proton. The synthesis of compound 4 and 5 was per formed by the reaction of compound (**3**) with ammonium thiocyanate for compound (**4**) or phenyl isocyanate for compound (**5**) (Scheme-3), and the products **4** and **5** were characterized by their physical and spectral data.

IR spectra of the compounds **4** and **5** showed NH stretching bands between 3380 and 3252 cm^{-1} and absorption bands for C=O (1690 and 1695 cm^{-1})and for C=S groups (1210 and 1220 cm^{-1}). In the ^{1}HNMR spectra of the compounds **4** and **5** the NH proton absorptions are appeared as singlets at δ 8.85 and 10.56 ppm, respectively.

The intramolecular cyclization of compounds **4** and **5** (Scheme 3) was performed by alkaline treatment of these intermediates under reflux conditions. It is well know that in case of these type of compounds thion-mercapto tautamerism can be occurred (**6** and **7**) and the SH signal due to thiol form is a more defined singlet than the NH signal diarized from triplets observed.[24,25]

The ^{1}HNMR spectra of the compounds **6** and **9** show the expected chemical shifts (Table 2). In the IR spectrum of 6 and 9 the stretching bands representing NH at 3314 and 3268 cm^{-1} are appeared and the signals due to C=O group are absent. The cyclization of compounds **4** and **5** in acidic medium yielded the compounds **7** and **8**. In the IR spectrum of compounds **7** and **8** the stretching bands due to NH at 3365 and 3215 cm^{-1} are appeared and the signal sdue to C=O group are completely absent.

The ^{1}HNMR spectra of compounds **5** and **10** contain the expected chemical shifts (Table 2). The thiosemicarbazide (**5**) was treated with mercuric oxide in methanol to give substituted 1,3,4-oxadiazole (**10**) derivative. The IR spectra of the compound 10 shows absorption bands at 3380 cm^{-1} , 1605 cm^{-1} and at 1210 cm^{-1} for NH, C=N and C-O-C linkages, respectively. In order to perform the synthesis of monosubstituted oxadiazole, the acid hydrazide (**3**) was treated with formic acid to give 2-chloro-N-formyl-1,8-naphthyridine-3-carbohydrazide **(11)** which was transformed into substituted 1,3,4-oxadiazole (**13**) in a reaction with PbO_2 (Table 2). The compound **11** showed absorption bands at 1715 cm^{-1} and 1653 cm^{-1} for C=O and a band at 1585 cm^{-1} for C=N group, furthermore two bands at 3380 and 3315 cm^{-1} for NH and a band at 2815 cm^{-1} for aldehyde group.

The ^{1}H NMR spectrum of compound **11** showed singlet at δ 4.85 for NH and a group of signals at δ 7.21-7.29 belong to phenyl ring and a triplet signal δ 7.33 for C-6, two doublet signals at δ 7.46 and 8.31 for C-5 and C-7, respectively and a signal at δ 7.81 for C-4. Compound **11** was cyclized by PbO_2 to give 2-substituted-1,3,4-oxadiazole (**13**). The IR spectrum of the compound **13** showed absorption bands at 1595 cm^{-1} for C=N and at 1085 cm^{-1} for C-O-C groups.

The ^{1}HNMR spectrum of the compound 13 contained the expected chemical shifts (Table 2) . The acid hydrazide (**3**) was treated with benzaldehyde to give hydrazone (**12**). The IR spectrum of the compound **12** showed IR absorption bands at 1675 cm^{-1} for C=O group and at 3325 cm^{-1} for NH group.

 DOI: 10.17628/ecb.2016.5.151-156

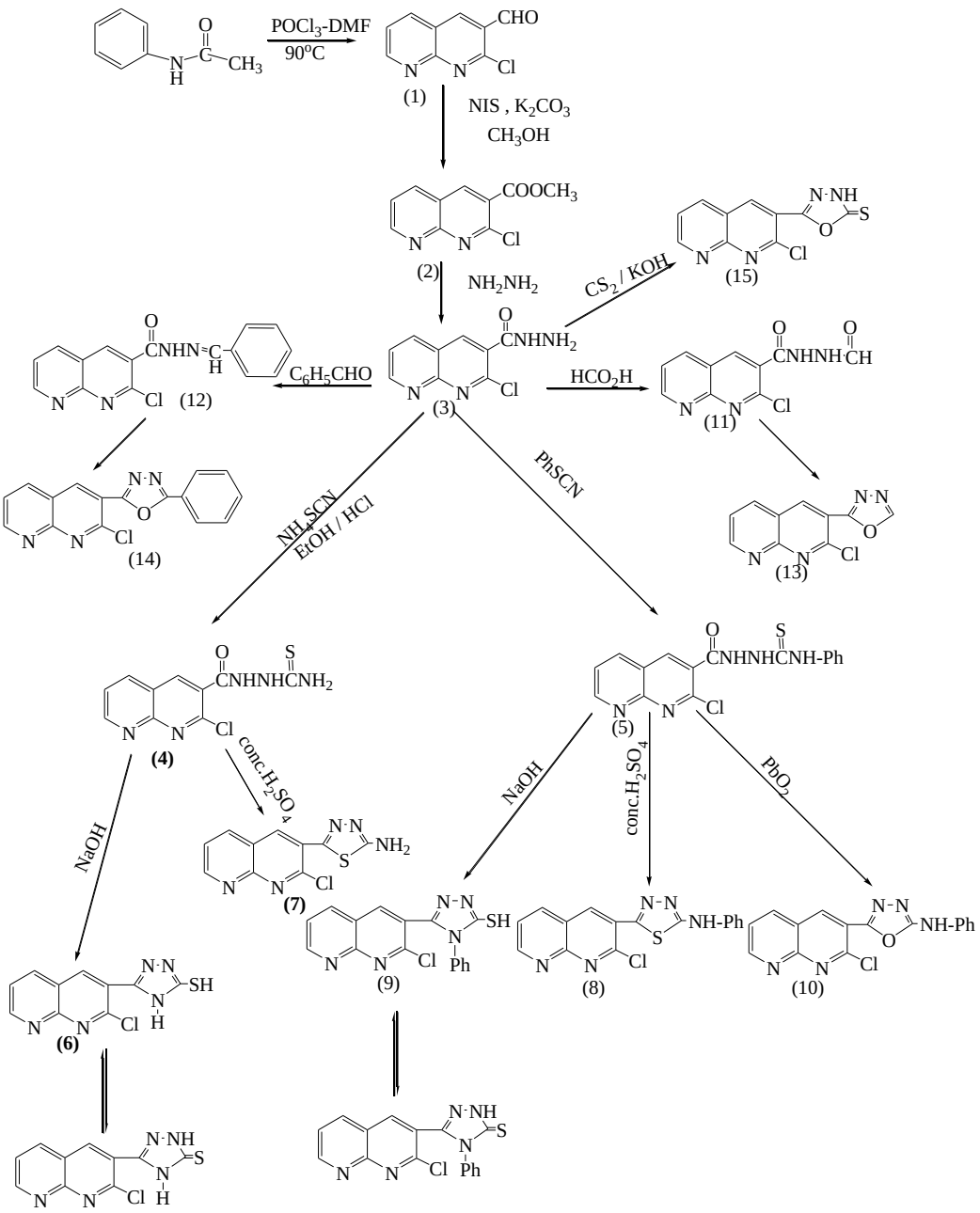

Scheme 3. A flow chart of synthesis of compounds (**1**) – (**15**).

The ^{1}H NMR spectrum of the compound **12** showed the NH signals at δ9.05 as a singlet. The hydrazone **12** was then cyclized to 2,5-disubstituted-1,3,4-oxadiazole (**14**) by PbO_2.

The compound **14** showed IR absorption at 1185 cm^{-1} for C-O-C and at 1605 cm^{-1} for C=N groups. The ^{1}H NMR of the compound **14** showed the expected chemical shifts (Table 2).

The base catalyzed cycle condensation of hydrazide (**3**) with carbon disulfide give 1,3,4-oxadiazole derivative (**15**) in good yield under reflux condition (Table 2) . The IR and ^{1}H NMR of these compound are listed in Table 1 and 2.

Biological activity.

The anti-microbial activity of compounds (**6**) **–** (**10**) and (**13**) – (**15**) were evaluated against *Eschershia Coli, Proteus Vulgaris, Staphylococcus Epidermidis* and *Staphylococcus Areus.* The results (Table 3) showed that these compounds have a good anti-microbial activity against *S. Aureus* and *S. Epidermidis*. Ciprofloxacin (Cipro) and chloramphenicol (Camph) were used as control. The concentration of the new compounds was 10 mg/disk while that of Cipro and Camph dose were selecdted to be 5 mg/disk and 39 mg/disk respectively.

 DOI: 10.17628/ecb.2016.5.151-156

Table 3. Antibacterial activity data of compound (6-10,13-15).

No.	Zone of inhibition in mm			
	S. Aureus	***S. Epidermidis***	***E. Coli***	***P. Vulgaris***
6	26	24	12	10
7	23	22	11	10
8	19	17	13	9
9	21	12	13	12
10	23	21	16	11
13	18	19	14	15
14	15	14	15	14
15	18	22	13	10
Cipro	-	-	15	14
Camph	17	16	14	-

CONCLUSION

In conclusion, we have developed a simple and efficient method for the synthesis of some new 1,8-naphthyridine derivatives and characterized them by spectral studies. Thenewly synthesized compounds (**6**, **7, 8**, **9**, **10**, **13**, **14** and **15**) were evaluated for their antibacterial activities. The results obtained indicated that these compounds had a good activity against *Staphylococcus aureus* and *Staphylococcus epidermidis*.

ACKNOWLEDGEMENT

The authors are thankful to Head, Department of Chemistry, Eskisehir Osmangazi University, Eskisehir, Turkey for providing ^{1}H NMR spectroscopy. We are also thankful to Head, Department of Biology, Mosul University for providing laboratory facilities.

REFERENCES

[1]Laxmlaayurt, E., Narender, A., Shera Shaurar, S., and Thirnmula chary, M., *Int. J. Appl. Chem*.**,** **2009**, *5*, 21.

[2]Thirumnal Chary, M., Laxmlaayurt, E., Shera Shaurar, S., and Narender, A., *Heterocycl. Commun*., **2009**, *15*, 35.

[3]Hagen, H., Pfister, J., Ziegler, K., Wuerzer, B., Westphalen, K. O., *Ger. Offen. DE 3907936*, **1991.**

[4]Serrakiui, P. L., Badawaen, M., Feunconi, F., Manera, C., Miealie, M., Meri, C., and Sdecomauni, G., *Farmaco*., **2001**, *56*, 311.

[5]Bamirbas, N., Alpaybarangle, S., Demirbas, A., and Sanent, K., Eur. *J. Med. Chem*., **2004**, *39*, 792-804.

[6]Amir, M., and Shikhu, K., *Sic. J. Med. Chem*., **2004**, *89*, 35-45.

[7]Kacahulkanli, A., Utes, O., and Atuk, G., *Farmaco*, **2001**, *56*, 493-499.

[8]Palaska, E., Saniu, G., Kelicen, P., Durlu, N. T., and Altnok, G., *Farmaco*, **2002**, *57*, 101-107.

[9]Palles, S., Gylery, N., and Piedeyle, H., *Farmaco*, **2002**, *57(2)*, 191-194.

[10]Merni, P., Zani, E., and Corrins, P., *Eur. J. Med. Chem*., **2002**, *9*, 651-654(part 2).

[11]Gorechi, D. K. J., Hawes, E. M., *J. Med. Chem.* **1973,** *20*, 124-128.

[12]Xia, Y., Chuan-Cong, F., Zhog, N., Chag, J., and Minom, S., *Eur. J. Med. Chem***.,** **2008**, *44*, 2147-2156.

[13]Melnyk, P., Leroux, V., Serghergert, C., and Grellier, P., *Bioorg. Med. Chem. Lett***.,** **2006**, *16*, 31-35.

[14]Sherif, A., and Rostom, F., *Bioorg. Med. Chem*., *2010*, *18*, 2767-2776.

[15]Bocharer, V. V., Ghidaspov, A. A., and Pereisdoua, E. V., *Chem. Heterocycl. Compd*., **2006**, *42*, 1096-1100.

[16]Mohareb, R. M., Ibrahim, R. A., and Mustafa, H. E., *Open Org. Chem***.,** **2010**, *4*, 8-14.

[17]Ranadheer, M., Laxmmarayana, E., Rainein, D., Sreeniuasulu, B., and Chary, M. T., *Int. J. Chem. Sci*., **2010**, *8(4)*, 2025-2030.

[18]Srivastava, A., and Singh, R. M., *Indian J. Chem*., **2005**, *44(B)*, 1868-1875.

[19]Mohanad, Y. S., and Ala, I. A., *Eur. J. Chem***.,** **2014,** *5(3)*, 475-480.

[20]Braccio, M. D., Grossi, G., Roma, G., Peras, D., Mattiali, F., and Eosmar, M., *Eur. J. Med.Chem***.,** **2008**, *43*, 584-594.

[21]Rul, G. A., Knmar, N. S., and Rajesdrou, S. P., *Asian J. Chem*., **2002**, *14*, 1303-1306.

[22]Ayoob, A. I., *J. Baghdad Sci.*, **2013**, *10(3)*, 758-764.

[23]Laracx, R. C., in "*Comprehensive organic transformations A Guide to Functional group preparation*s", (Velt Publications , NC-York), **1989**, 840.

[24]Bayrak, H., Demirbas, A., Demjrbas, N., and Alpaykaraoglu, S., *Eur.J. Med.Chem***.,** **2010**, *45*, 4726-4732.

[25]Bayrak, H., Demirbas, A., Bektas, H., Alpaykaraoglu, S., and Demirbas, N., *Turk. J. Chem***.,** **2010**, *34*, 835-846.

Received: 29.05.2016.
Accepted: 25.06.2016.

 DOI: 10.17628/ecb.2016.5.151-156